SYNTHESIS AND CHARACTERIZATION OF SnTe$_{0.5}$ Se$_{0.5}$ MATERIAL FOR THERMOELECTRIC APPLICATION

Submitted in partial fulfillment of the requirements for the award of Master of Science degree in Physics

By

Tisha Jafrin. S (40590007)

DEPARTMENT OF PHYSICS

SCHOOL OF SCIENCE AND HUMANITIES

SATHYABAMA
INSTITUTE OF SCIENCE AND TECHNOLOGY
(DEEMED TO BE UNIVERSITY)

Accredited with Grade "A" by NAAC
JEPPIAAR NAGAR, RAJIV GANDHI SALAI, CHENNAI - 600 119

MAY – 2022

SATHYABAMA
INSTITUTE OF SCIENCE AND TECHNOLOGY
(DEEMED TO BE UNIVERSITY)
Accredited "A" Grade by NAAC | 12B Status by UGC | Approved by AICTE
www.sathyabama.ac.in

DEPARTMENT OF PHYSICS

BONAFIDE CERTIFICATE

This is to certify that this Project Report is the bonafide work of **TISHA JAFRIN. S (40590007)** who carried out the project entitled "**Synthesis and Characterization of $SnTe_{0.5}$ $Se_{0.5}$ material for thermoelectric application** " under my supervision from **NOVEMBER 2021 TO MARCH 2022**

Internal Guide & Head of the Department
Dr. S. RAVICHANDRAN, M.Sc., M.Phil., Ph.D

Submitted for Viva voce Examination held on______________________

Internal Examiner **External Examiner**

DECLARATION

I **Tisha Jafrin.S (40590007)** hereby declare that the Project Report entitled **“Synthesis and Characterization of $SnTe_{0.5}$ $Se_{0.5}$ material for thermoelectric application**” done under the guidance of **Dr. S. Ravichandran** is submitted in partial fulfillment of the requirements for the award of Master of Science degree in Physics.

DATE:

PLACE: **SIGNATURE OF THE CANDIDATE**

ACKNOWLEDGEMENT

I am pleased to acknowledge my sincere thanks to Board of Management of **SATHYABAMA** for their kind encouragement in doing this project and for completing it successfully. I am grateful to them.

I convey my thanks to Dean, School of Science and Humanities and **Dr. S. RAVICHANDRAN M.Sc., M.Phil., Ph.D.,** Professor & Head of the Department, Dept. of Physics for providing me necessary support and details at the right time during the progressive reviews.

I would like to express my sincere and deep sense of gratitude to my Project Guide for his valuable guidance, suggestions and constant encouragement paved way for the successful completion of my project work.

I wish to express my thanks to all Teaching and Non-teaching staff members of the Department of Physics who were helpful in anyways for the completion of the project.

TISHA JAFRIN S

ABSTRACT

The environmentally friendly thermoelectric materials has been attracted considerable towards the SnTe materials. In this project, SnTe is the parent material and the Se is considered to be the dopant material. Here the combination of SnTe0.5 Se0.5 material is being taken and synthesized by the ball milling method at room temperature to study the thermoelectric properties of the sample.

After that the sample is made as a pellet using the peletizer for the futher studies. Then the sample were characterized by the X-Ray diffraction(XRD), Scanning Electron Microscope(SEM) with EDAX and Hall effect measurement respectively to analysis the morphological and phase of the material. The hall effect measurement shows that the SnTe0.5 Se0.5 material is a n-type material.

The figure of merit should be maintained to be a efficient thermoelectric material. High seeback coefficient, electrical conductivity and low thermal conductivity is needed for a proper and good efficiency. Further in future the material will be implemented in the various thermoelectric application field due to it high thermoelectric properties.

TABLE OF CONTENT

LIST OF TABLES

LIST OF FIGURES

LIST OF SYMBOLS AND ABBREVIATIONS

Sn	Tin
Te	Tellurium
Se	Selenium
XRD	X-Ray Diffraction
SEM	Scanning Electron Microscope
EDAX	Energy Dispersive X-ray Analysis
TE	Thermoelectric
Emf	Electromotive force
TEGs	Thermoelectric generators
HMS	Health Monitoring System
CaTe	Calcium Telluride
CHP	Combined Heat and Power
Bi_2Te_3	Bismuth Telluride
Cu_2Se	Copper Selenide
Ppm	parts per million
TEM	Transmission Electron Microscope

Greek Letters

σ	Electrical conductivity
T	Absolute temperature
S	Seebeck coefficient
K	Thermal conductivity
Kc	Carrier thermal conductivity
Kl	Lattice thermal conductivity
D	Crystalline size

CHAPTER 1

INTRODUCTION

1.1 THERMOELECTRIC INTRODUCTION:

Thermoelectric (TE) materials are particularly intriguing because they can convert heat to electricity and vice versa in the presence of a temperature gradient. They have a lot of promise because of their ability to play a part in the future of energy efficiency. In order to considerably increase the thermoelectric performance of materials, many ways have been used. Energy materials, such as thermoelectric materials with higher efficiency, will play an essential role in energy storage, conversion, recovery, and transport. Automotive waste heat power production, direct solar thermal energy conversion, and superconducting electronics are some of the new and exciting applications of thermoelectric materials. All of these applications demand novel and enhanced thermoelectric materials with improved performance, chemical and thermal stability, and environmental safety at the required operating temperatures. The conversion of heat energy into electricity is one of the most important components of thermoelectrics. The goal of this thesis is to create a material for thermoelectric application and analyse its characterization.

1.2 THERMOELECTRIC HISTORY:

Allesandro Volta, an Italian scientist, discovered in 1794 that a metal rod with two ends at differing temperatures caused frog muscles to spasm. Thomas Johann Seebeck found the same phenomena in 1822 when he noticed the deflection of a compass needle when it came near to two metal junctions held at different temperatures. The Seebeck effect (generating a voltage from a temperature differential), Peltier effect (driving heat flow with an electric current), and Thomson effect are all used in these thermoelectric materials (Reversible heating or cooling in the conductor when both current and temperature gradients are present). The Seebeck effect occurs when a temperature differential between two dissimilar electrical conductors or semiconductors results in a voltage difference between them. The Peltier effect is the inverse of the Seebeck phenomenon. When an electric current travels through a junction between two materials, the Peltier effect causes heat to be emitted or absorbed. Heat is developed or absorbed throughout the length of an unequally heated conductor when a current passes through it, depending on the direction of the current flow. The Thomson effect is the name of this phenomenon. This is a reversible effect.

1.3 EFFECT OF THERMOELECTRIC:

The thermoelectric energy element is stated for a thermoelectric material, given

Power factor= $\sigma S^2 [W/m/K^2]$

where S means Seebeck coefficient and

σ means electrical conductivity.

TE devices with higher power factor materials can "generate" more energy.

The thermoelectric effect is the use of thermocouples to convert temperature changes into voltages and vice versa. The non-dimensional figure-of-merit determines the efficiency of thermoelectric power generators.

$$ZT=S^2\sigma T/k,$$

where S is the Seebeck coefficient,

σ the electrical conductivity,

k the thermal conductivity,

and T the absolute temperature.

The thermal conductivity is represented as

$$k = klatt + kcarrier,$$

where klatt represents the lattice thermal conductivity owing to lattice vibrations and kcarrier represents the electronic thermal conductivity due to carriers.

Increasing the electrical characteristics S2 or reducing the thermal conductivity are the two main ways to improve thermoelectric performance. Materials having high electrical conductivity, low thermal conductivity, and a high Seebeck coefficient are required for high efficiency. The difficulty in detecting the applied temperature differential among thermoelectric devices makes thermoelectric performance measurement problematic. Comparing various thermoelectric performance statistics requires careful study. Bismuth telluride is the most often used thermoelectric material (Bi2Te3).

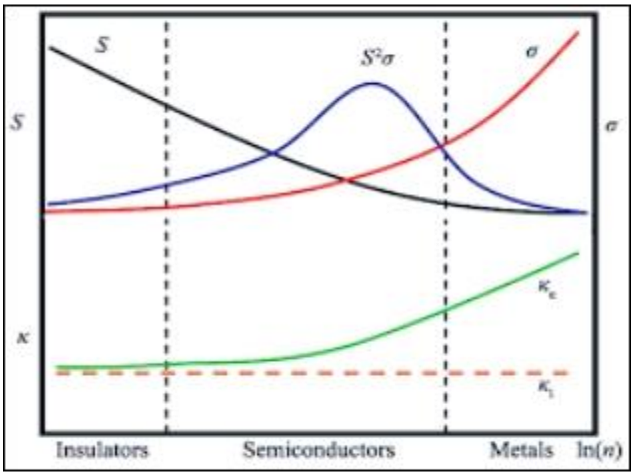

Fig. 1.1 Relationship between α, σ, k, Power Factor, zT and Carrier Concentration

Seebeck effect, Peltier effect, and **Thomson effect** are the three essential effects for thermoelectric characteristics. When two junctions are kept at different temperatures, the Seebeck effect produces an electromotive force (emf) and an electric current in a loop of material consisting of at least two dissimilar conductors. **The Seebeck effect** is used to produce electric power for particular purposes and to detect temperature with high sensitivity and precision (see thermocouple). The Seebeck emf (or thermo/thermal/thermoelectric emf) is the name of the emf. The Seebeck coefficient is the ratio of electromotive force to temperature difference. **The Peltier effect** is the inverse of the Seebeck effect, in which an electrical current passing through a junction connecting two materials emits or absorbs heat per unit time at the junction to equalize the difference in chemical potential between the two materials. The Peltier coefficients indicate the amount of heat transported per unit charge. The Peltier cooler is an electrical refrigerator that may be built. If the temperatures of the two points in the conductor are different, these points will be different, resulting in a potential difference between these points. This is known as the **Thomson effect**. Thomson effect is also reversible.

1.4 APPLICATION OF THERMOELECTRIC MATERIALS:

1.4.1 Refrigeration:

The thermoelectric material can be used as a refrigerator known as a "thermoelectric cooler" or "Peltier cooler" after the Peltier effect that drives the operation. As a freezing technique, Pelche cooling is much less common than steam compression cooling. The main advantages of Pelche coolers (compared to vapor-compression refrigerators) are the absence of moving parts and refrigerants, their small size and their flexibility in shape (form factor). The main drawback of Pelche coolers is their inefficiency. It is estimated that most applications will require materials with ZT> 3 (efficiency of about 20-30 μm) to replace traditional coolers. Currently, Pelche coolers are only used in niche applications, especially small ones where efficiency is not an issue.

1.4.2 Power generation:

Thermoelectric efficiency depends on (ZT)figure of merit. ZT has no theoretical upper limit, and as ZT approaches infinity, thermoelectric efficiency approaches the Carnot limit. However, until recently, there was no known thermoelectric element with ZT> 3. In 2019, researchers reported about 5-6 materials for ZT. As of 2010, thermoelectric generators are useful for niche applications where efficiency and cost are less important than reliability, light weight, and small size. The internal combustion engine detects 20-25% of the energy released during fuel combustion. The conversion of conversion can increase kilometers and power onboard control elements and creature comfort (stability management, telematics, navigation system, electronic brake, etc.). It may be possible to reduce energy from the engine (in some cases) the electrical load of the vehicle. Electric power steering or electric coolant pump operation. The CHP power plant uses heat generated during power generation for alternative purposes. This is in the industry with high levels of waste energy. Thermal electricity can correspond to applications in such systems or solar thermal energy generation.

Thermoelectric materials can be used for heating/cooling purposes, or for power generation. The applications for thermoelectric materials can span different areas and industries. Generating energy from waste heat in the automotive industry is a promising application of such technology.

1.5 ADVANTAGES OF THERMOELECTRIC MATERIALS

Thermoelectric materials are used in niche cooling applications, for example, maintaining very stable temperatures in lasers and photodetectors, and are commonly found in office water coolers. They are also used in space exploration to convert heat from radioactive materials into electricity. And it has, high electrical conductivity, continuous power output, machinability, stable, high seebeck coefficient, low thermal conductivity, soft and cheap

1.6 DISADVANTAGES OF THERMOELECTRIC MATERIALS

Here are some disadvantages of Thermoelectric materials, such that low seebeck coefficient

CHAPTER 2

LITERATURE SURVEY

In 2020, Guo, Xuming et al. were studied thermoelectric transport properties in Bi-doped SnTe, SnSe alloys. The purpose of this study was to alloying trivalent Bi or chalcogenide SnSe alone in SnTe can trigger an inherent enhancement of thermoelectric performance and particularly, fully evaluating the effect of band convergence on carrier concentration-dependent weighted mobility..

In 2020, Jiang, Qinghui et al. studied high thermoelectric performance in SnTe nanocomposites with all scale hierarchical structures. The purpose of this study was to the practical realization of SnTe nanostructured composites is often limited by long reaction time, low yield and aggregation of nanoparticles and A simple substitution reaction between Cu2Se and SnTe was used to achieve a Cu1.75TeSnTe nanocomposite with a unique hierarchical structure at all scales.

In 2011, Fa Y.Y. Wang et al. were studied facile synthesis and characterization of SnTe films. This purpose of this study was to the films were prepared by a chemical bath method, at room temperature and ambient pressure, using conventional chemicals as starting materials with or without surfactant and the films were characterized by X-ray diffraction, X-ray photoelectron spectroscopy and field-emission scanning electron microscopy, respectively.

In 2018, Wang, Wen-ting et al. were studied synthesis process and thermoelectric properties of n-type tin selenide thin films. The purpose of this study was to n-type SnSe thin films were synthesized via thermal evaporation using powdered SnSe that was prepared directly by mechanical alloying and the thermoelectric step improved the crystallinity of the film, which improved the properties of the film.

In 2019, Witting, I. T., et al. studied the thermoelectric Properties of Bismuth Telluride. The purpose of this study was to the minority carrier excitation across the small bandgap significantly limits the thermoelectric performance of Bi_2Te_3, even at room temperature, showing that larger bandgap alloy is required for high temperature operation.

In 2011, Saleemi, Mohsin; et al. were studied synthesis, processing and thermoelectric properties of bulk nanostructured bismuth telluride. The purpose of this study was to its dimensionless figure-of-merit-*ZT* around 1 limit the large-scale industrial applications. Recent studies indicate that nano-structuring can enhance *ZT* while keeping the material form of *bulk* by employing an advanced synthetic process accompanied with novel consolidation techniques.

In 2021, Manjula, M., et al. studied influence of Ternary and Quaternary Inclusion on Bandgap Tuning of CaTe: Prediction of Potential Thermoelectric Materials. The purpose of this paper to study was CaTe, $Ca_{0.5}Ba_{0.5}Te$, $CaTe_{0.5}Se_{0.5}$, and $Ca_{0.5}Ba_{0.5}Te_{0.5}Se_{0.5}$ alloys structural, optoelectronic, and thermoelectric properties are studied using the full-potential linearized augmented plane wave method within the framework of density functional theory.

In 2018, Du, Y., et al. studied flexible thermoelectric materials and devices. The purpose of this study was to review the research progress on flexible thermoelectric materials and generators, including theoretical principles for TEGs, conducting polymer TE materials, nanocomposites comprised of Inorganic nanostructures in polymer matrices and all-inorganic flexible TE materials in nanostructured thin films.

In 2019, Wolf, M., et al. studied high Power Factor vs. HighzT-Overview of thermoelectric materials for high temperature applications. The purpose of this study was to revitalize Ioffe plots as a useful tool for making the thermoelectric properties of a material obvious and these plots enable us to Consider not only the efficiency of the material by the figure of merit zT, but also the power factor and the entropy conductivity as separate parameters.

CHAPTER – 3

AIM AND SCOPE OF THE PRESENT INVESTIGATION

3.1 AIM

The aim of the project is to synthesis and characterize the high-efficient thermoelectric material. It has a high scope due to their potential in playing a vital role in the future of energy efficiency. To increase efficiency, materials with high electrical conductivity, low thermal conductivity, and high Seebeck coefficient are required.

This thesis focuses on the synthesis and characterization of a Se doped SnTe thermoelectric materials by ball milling method. Further, the characterization of the materials is studied for analyzing the materials for the future thermoelectric applications. The main focus of this project is to develop the new thermoelectric material experimentally with the help of theoretical results.

In this study, the SnTe taken as the parent material and Se has considered as the dopant material. The SnTe0.5 Se0.5 combination of materials are taken and we have tried to synthesis a material for thermoelectric application. From the hall effect measurement, the synthesized material $SnTe_{0.5}Se_{0.5}$ is found n-type material. The result and discussion section deals with the experimental and characterization of this thermoelectric materials by analyzing SEM, XRD and Hall co-efficient.

The areas of application of thermoelectric materials are automotive waste heat power generation, direct solar thermal energy conversion, and superconducting electronics. And the present thermoelectric application was in cookware. The scope of the thesis is for thermoelectric application with high figure of merit. And producing and discovering thermoelectric products for the use of human being in daily life.

3.2 SCOPE:

The scope of thermoelectric materials was in military, space vehicles, consumer wearables, industrial , automotive and residential. Military avionics, infrared detectors, thermal imaging devices, cooling systems, and missile tests are just a few examples of military applications where thermoelectric generation is very important potential and huge promise.

Thermoelectric energy harvesting is used in space vehicles where replying on batteries to power devices is not very practical. Thermoelectric energy harvesting is also used in aircraft health monitoring systems (HMS).

In recent years, wearables have exploded. Smart watches, fitness trackers and more have become an integral part of people's daily lives. Thermoelectric system could be mounted on domestic boilers, water heaters, stoves or even solar energy systems.

Thermoelectric materials are placed in the exhaust system of an automobiles should theoretically be able to harvest enough energy to at least play an augmenting role to the battery. Residential thermoelectric generators have a wide range of applications for powering all types of smart home devices, including: Smart light switch, smart refrigerator, smart bulbs etc.

Therefore, in the same way the material synthesized has expected to replace the convenient efficient thermoelectric materials in commercial process. This material is being expected to have a high scope in the future application by performing a high efficient thermoelectric properties.

CHAPTER 4

SELECTION OF MATERIALS AND METHODS

4.1 TELLURIUM

Tellurium is a metalloid, luster, crystalline, brittle, silvery white element. It is usually available as a dark gray powder. It has both metallic and non-metallic properties. Tellurium forms many compounds similar to sulfur and selenium. When burned in the air, tellurium has a greenish-blue flame, thereby forming tellurium dioxide. Telluriumis not affected by water or hydrochloric acid, but dissolves in nitric acid.

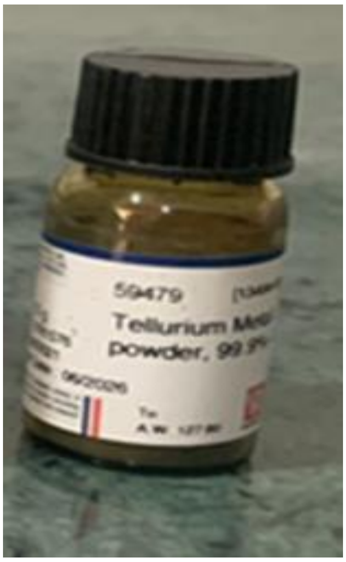

Fig.4.1. Pure Tellurium metal powder

4.1.1 TELLURIUM IN THE ENVIRONMEMT

Tellurium is present in coal up to 2 ppm. This is probably the main source of this metal that plants can absorb from the soil. Tellurium in plants can reach up to 6 ppm, but few food plants exceed 0.5 ppm and are mostly less than 0.05 ppm. Unbound tellurium samples may be found, but very rarely. There are some tellurium minerals (caravelite, sylvanite, tellurium), but none have been mined as a source of elements.

World production is around 220 tonnes/year. The main producing countries are the United States, Canada, Peru and Japan. The reserves of this element have not been evaluated.

4.1.2 HEALTH EFFECTS OF TELLURIUM:

Fortunately, tellurium compounds are rarely encountered by most people. They are teratogenic and ought to best be treated via way of means of capable chemists due to the fact that ingestion in even small quantities reasons dreadful smelling breath and appalling frame odour.

4.1.2.1 ROUTES OF EXPOSURE:

Absorption into the body by inhalation of aerosol.

4.1.2.2 INHALATION RISK:

Evaporation at 20 ° C is negligible. However, when dispersed, it can quickly reach harmful particle concentrations in the air. Effects of inhalation: Drowsiness. Dry mouth. Metal taste. Headache. Garlic odour. Nausea.

4.1.2.3 EFFECTS OF SHORT-TERM EXPOSURE:

Aerosols of this substance irritate the eyes and airways. This substance can affect the liver and central nervous system. Exposure may result in garlic-like breath. Medical observation is indicated. Ingestion: Abdominal pain. Constipation. Vomiting.

4.1.2.4 CHEMICAL DANGERS:

Upon heating, toxic fumes are formed. It reacts violently with halogens or interhalogen compounds and poses a fire hazard. Reacts with zinc with incandescence. Lithium silicide attacks tellurium with incandescence. Combustible. The finely dispersed particles form an explosive mixture in the air.

4.1.3 ENVIRONMENTAL EFFECTS OF TELLURIUM

Not harmful by natural processes or easily harmless. When heated to decomposition, tellurium chloride can emit toxic tellurium and chlorine smoke.

4.1.4 CHEMICAL PROPERTIES OF TELLURIUM

Atomic number	52
Atomic mass	127.6 $g.mol^{-1}$

Electronegativity according to Pauling	2.1
Density	6.24 g.cm^{-3}
Melting point	450 °C
Boiling point	988 °C
Vanderwaals radius	0.137 nm
Ionic radius	0.221 nm (-2) ; 0.089 nm (+4)
Isotopes	23
Electronic shell	[Kr] $4d^{10}$ $5s^{2}5p^{4}$
Energy of first ionization	869.0 kJ.mol^{-1}
Standard potential	0.91 V (Sb^{3+}/ Sb)

Discovered by-Franz Muller von Reichenstein in 1782

4.1.5 APPLICATIONS OF TELLURIUM

Tellurium is often used as an additive to steel and is often alloyed with aluminum, copper, tin, or lead. Tellurium is added to improve durability, strength and corrosion resistance. It can be used for cast iron, ceramics, detonator caps, solar panels, and chalcogenide glass. Adding tellurium to rubber speeds up the curing process, makes the product less susceptible to aging and less susceptible to the oils that soften regular rubber.

4.2 SELENIUM

Selenium is a non-metallic chemical element and is a member of Group XVI in the Periodic Table. In chemical activity and physical properties, it is similar to sulfur and tellurium. Selenium appears in a number of allotropic forms: the most popular are a red amorphous powder, a red crystalline material, and a grey crystalline metallise form called *metallic* selenium. The latter form conducts electricity better in the light than in the dark and is used in photocells. Selenium burns in the air and is not affected by water, but is soluble in concentrated nitric acid and alkalis.

Fig.4.2. Pure selenium metal powder

4.2.1 SELENIUM IN THE ENVIRONMENT:

Selenium is one of the rarer elements on the surface of this planet than silver. Selenium is generated in the atmosphere as a methyl derivative. Uncombines selenium is occasionally found and there are around 40 known selenium-containing minerals, some of which can have as much as 30% selenium - but all are rare and Generally, they occur with sulfides of metals such as copper, zinc and lead. The most important producing countries are Canada, the United States, Bolivia and Russia. The world's industrial production of selenium is about 1500 tons per year, and about 150 tons of selenium are recycled from industrial waste and recovered from old copy machines.

Selenium occurs naturally in the environment. It is released by both natural processes and human activity. Well-fertilized agricultural soil is generally about 400 mg / ton due to the natural presence of elements in phosphate fertilizers. Ans are often added as micronutrients. In its natural form as an element, selenium cannot be formed or destroyed, but selenium has the ability to change its shape.

Selenium levels in soil and water are rising as selenium precipitates in the air and selenium from waste also tends to invade the soil of landfills. When selenium does not react with oxygen in the soil, it remains fairly immobile. Selenium, which is immobile and insoluble in water, has a low risk to living organisms, and the oxygen level of the soil and the acidity of the soil increase the morphology of selenium that can be moved. Higher oxygen levels and acidity of soil are usually caused by human activities such as industrial and agricultural processes. The higher the mobility of selenium, the greater the likelihood of exposure to the compound. Soil temperature, moisture, water-soluble selenium concentration, timing, organic content, and microbial activity determine the rate at which selenium travels through the soil. In other words, these elements determine its mobility.

Agriculture not only raises soil selenium levels, but when selenium is introduced into irrigation drains, selenium concentrations in surface water can increase.

4.2.2 HEALTH EFFECTS OF SELENIUM

People can be exposed to selenium in a variety of ways. Exposure to selenium occurs through food and water, or when in contact with soil or air containing high concentrations of selenium. This is not surprising as selenium is naturally abundant in the environment and is very widespread. Exposure to selenium is primarily through food, as selenium is naturally found in grains, grains and meat. Humans must take a certain amount of selenium daily to stay healthy. Foods usually contain enough selenium to prevent deficiency. In the past, many selenium-rich fertilizers have been applied to farmlands, so in many cases selenium dietary intake can be higher than normal. People living near hazardous waste sites are exposed to higher soil and air pollution. Selenium from dangerous landfills and farmlands flows into groundwater and surface water by irrigation.

This phenomenon causes selenium to seep into local drinking water, temporarily increasing water exposure to selenium. People working in the metal, selenium recovery, and paint industries tend to be exposed to higher levels of selenium, primarily through breathing. Selenium is released into the atmosphere by burning coal and oil. People who eat large amounts of grains that grow near industrial lands may have high dietary exposure to selenium.

Exposure to selenium through drinking water may be increased when selenium from hazardous waste disposals ends up in water wells.Exposure to selenium through air only comes about in the workplace usually. It can cause dizziness, malaise and inflammation of the mucous membranes. Extremely high exposure can cause water buildup in the lungs and bronchitis. Dietary selenium intake is usually sufficient to meet human needs. Bottlenecks rarely occur. When a deficiency occurs, heart and muscle problems can occur. Too much selenium intake can have health consequences.

The severity of these effects depends on the concentration of selenium in the food and how often the food is eaten. The health effects of various forms of selenium range from brittle hair and deformed nails to skin rashes, fever, swelling and severe pain. When selenium gets into your eyes, it causes a burning sensation, irritation, and tears. In some cases, selenium poisoning can be very serious and even fatal.

Excessive exposure to selenium vapor is lung, garlic breath, bronchitis, pneumonia, bronchial asthma, nausea, cold, fever, headache, sore throat, shortness of breath, conjunctivitis, vomiting, abdominal pain, diarrhea, and liver. It can cause bloating. Selenium is an eye and upper respiratory tract stimulant and sensitizer. Overexposure can cause red discoloration of the nails, teeth and hair. Selenium dioxide reacts with water to form corrosive acids, which are corrosive to the skin and eyes. Carcinogenicity The International Agency for Research on Cancer (IARC) lists selenium in Group 3 (this substance is not classified as carcinogenic to humans).

4.2.3 EFFECTS OF SELENIUM ON THE ENVIRONMENT:

Small amounts of selenium can invade soil and water due to weathering of rocks. After that, when it is taken up by plants or adsorbed by fine dust, it floats in the air. Selenium is most likely released into the atmosphere as selenium dioxide from the burning of coal and petroleum. This substance is converted to selenic acid by water and sweat. Selenium substances in the air usually break down fairly quickly into selenium and water, so they do not pose a danger to the health of the organism.

The behavior of selenium in the environment is highly dependent on its interaction with other compounds and the environmental conditions at a particular location and at a particular time. There is evidence that selenium can accumulate in the body tissues of living organisms and cross the food chain. This biological increase in selenium usually begins when the animal eats many plants that have absorbed large amounts of selenium before digestion. Due to irrigation spills, aquatic selenium concentrations tend to be very high in many areas. Absorption or accumulation of very high concentrations of selenium in animals can cause reproductive disorders and birth defects.

4.2.4 PROPERTIES OF SELENIUM

Atomic number	34
Atomic mass	78.96 g.mol $^{-1}$
Electronegativity according to Pauling	2.4
Density	4.79 g.cm^{-3} at 20°C
Melting point	217 °C
Boiling point	688 °C
Vanderwaals radius	0.14 nm
Ionic radius	0.198 nm (-2) ; 0.042 nm (+6)
Isotopes	9
Electronic shell	[Ar] 3d^{10} 4s^{2} 4p^{4}
Energy of first ionization	940,7 kJ.mol $^{-1}$
Energy of second ionisation	2045 kJ.mol $^{-1}$
Energy of third ionisation	2973.7 kJ.mol $^{-1}$
Standard potential	0.77 V

Discovered by-Jons Berzelius 1817

4.2.5 APPLICATIONS OF SELENIUM:

Selenium has excellent photovoltaic and photoconductivity properties and is widely used in electronic devices such as photocells, light meters and solar cells. The second most common use of selenium is in the glass industry. Selenium is used to remove color from glass and give it a red color to glass and enamel. The third min use, taking about 15% is sodium selenite for animal feeds and food supplements. Selenium can also be used for photo copying and toning. Its artistic use helps enhance and magnify the tonal range of black-and-white photographs. Other uses for selenium are found in metal alloys such as lead plates used to convert alternating current to direct current in batteries and rectifiers. Selenium is used to improve the wear resistance of vulcanized rubber. Some selenium compounds are added to the anti-dandruff shampoo.

4.3 TIN

Tin is a soft, pliable, silvery-white metal. Since tin is protected by an oxide film, it is difficult to oxidize and has corrosion resistance. Tin resists corrosion from distilled seawater and soft tap water and can be attacked by strong acids, strong bases and acid salts.

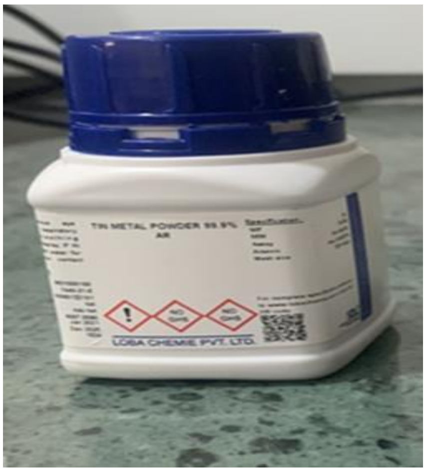

Fig.4.3. Pure Tin metal powder

4.3.1 *TIN IN THE ENVIRONMENT*

Tin oxide is insoluble and the ore is highly weather resistant, resulting in low levels of tin in soil and natural water. Concentrations in soil are generally in the range of 14 ppm, but some soils are less than 0.1 ppm and peat can reach 300 ppm. There are few minerals that contain tin, but only one is commercially important, it is cassiterite.

The main mining area to be found in the *tin belt* which goes from China through Thailand, Brimah and Malaysia to the islands of Indonesia. Malaysia produces 40% of the world's tin. Bolivia and Brazil are the other important tin mining areas. Global production exceeds 140,000 tonnes annually and available reserves exceed 4 million tonnes. Tin concentrates are produces in around 130.000 tonnes per year.

4.3.2 HEALTH EFFECTS OF TIN:

TIN is mainly applied in various organic substances. The most dangerous form of tin for humans are the organic tin bonds Although dangerous, it is used in a wide range of industries, including the paint and plastic industries, as well as in pesticide-mediated agriculture. Although the effects of tin poisoning are known, the use of organotin substances continues to increase.

The effects of organic tin substances can vary. They depend on the type of substance present and the organisms exposed to it. Triethyltin is the most dangerous organotin substance for humans. Hydrogen bonds are relatively short. The longer hydrogen bonds, the less dangerous tin substances are to human health. Humans can absorb tin compounds not only through the skin, but also through food and breathing. Ingestion of tin bonds can produce both acute and long-term effects.

Acute effects are:
- Eye and skin irritations
- Headaches
- Stomach-aches
- Sickness and dizziness
- Severe sweating
- Breathlessness
- Urination problems

Long-term effects are:
- Depressions
- Liver damage
- Malfunctioning of immune systems
- Chromosomal damage
- Shortage of red blood cells
- Brain damage (causes of anger, sleep disorders, oblivion, headaches)

4.3.3 EFFECTS OF TIN ON THE ENVIRONMENT

Tin as an individual atom or molecule is less toxic to any type of organism, and its toxic form is organic. Organic tin components can remain in the environment for long periods of time. They are very durable and not biodegradable. Microorganisms are extremely difficult to break down organotin compounds that have accumulated at the bottom of the body of water over the years. This will further increase the concentration of organotin.

When organotin is adsorbed on mud particles, it can spread throughout the water system. They are highly toxic to fungi, algae and phytoplankton and are known to cause great harm to aquatic ecosystems. Phytoplankton is a very important link in aquatic ecosystems because it supplies oxygen to other aquatic organisms. It is also an important section of the aquatic food chain. There are many different types of organotin, and their toxicity varies greatly. Tributyltin is the most toxic tin component for fish and fungi, but triphenyltin is much more toxic to phytoplankton. Organic doses are known to disrupt aquatic growth, reproduction, enzymatic systems, and feeding patterns. Exposure is primarily in the uppermost aqueous layer, as organotin compounds accumulate there.

4.3.4 CHEMICAL PROPERTIES OF TIN

Atomic number	50
Atomic mass	118.69 g.mol $^{-1}$
Electronegativity according to Pauling	1.8
Density	5.77g.cm^{-3} (alpha) and 7.3 g.cm^{-3} at 20°C (beta)
Melting point	232 °C
Boiling point	2270 °C
Vanderwaals radius	0.162 nm

Ionic radius	0.112 nm (+2) ; 0.070 nm (+4)
Isotopes	20
Electronic shell	[Kr] $4d^{10}$ $5s^{2}5p^{2}$
Energy of first ionization	708.4 $kJ.mol^{-1}$
Energy of second ionization	1411.4 $kJ.mol^{-1}$
Energy of third ionization	2942.2 $kJ.mol^{-1}$
Energy of fourth ionization	3929.3 $kJ.mol^{-1}$
Discovered by	The ancients

4.3.5 APPLICATIONS OF TIN

Tin is used to coat the cans. Tin-plated steel containers are commonly used for food preservation. Tin alloys have many uses. Solder for joining pipes and electrical circuits, tin, bell metal, babbitt metal, dental amalgam, etc. Niobium-tin alloys are used in superconducting magnets, and tin oxides are used in ceramics and gas sensors (absorbing gas increases electrical conductivity and can be monitored). Tin foil was once a common food and pharmaceutical packaging material, but is now being replaced by the use of aluminum foil.

4.3.6 REASON FOR THE SELECTION OF THESE MATERIALS

All lead (Pb) based materials are toxic and dangerous to human being. It is used in paint and gasoline and is still used in batteries, solder, pipes, pottery, roofing materials and some cosmetics. Lead-free SnTe compound is an alternative material for PbTe with suitable band gap, non-toxic and mechanical stability. Narrow band gap semiconductor with high mobility charge carriers. These materials are operating at room temperature applications. Flexible material with good mechanical strength and low density. Doping is the one of the basic ways of tailoring properties of the IV-VI-based materials.

4.4 SELECTION OF SYNTHESIS METHOD

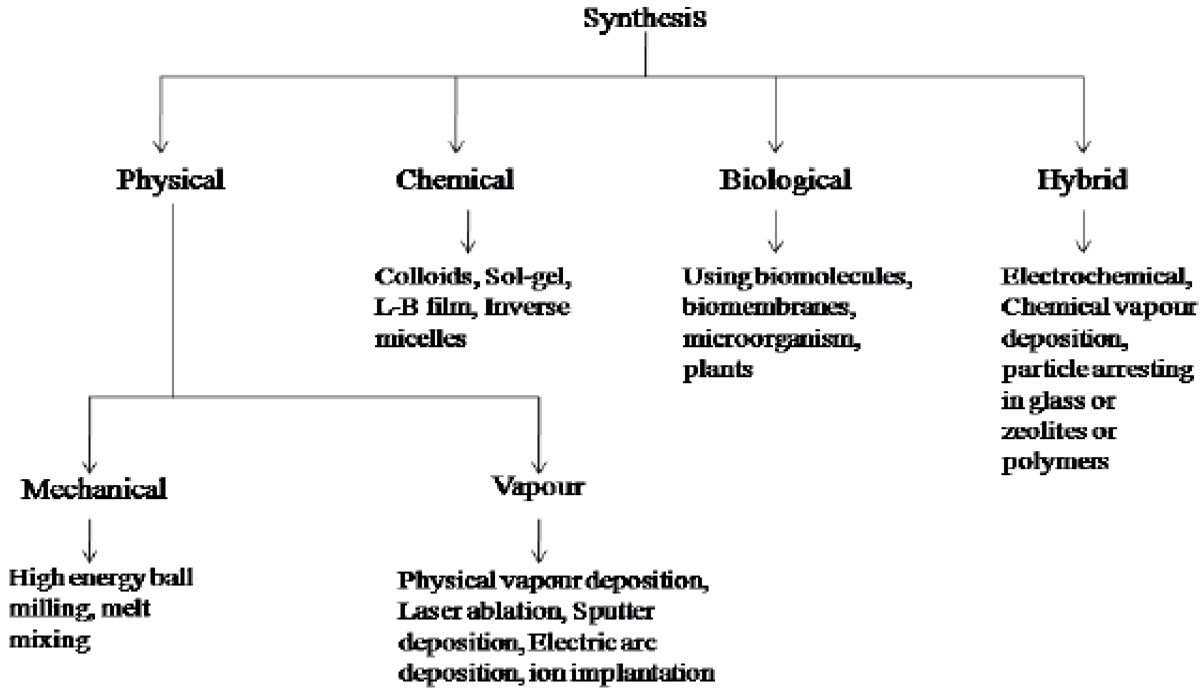

Fig.4.4 Flow chart of synthesis method

4.4.1 BALL MILLING METHOD:

- Ball milling is a grinding method that grinds nanotubes or powders into extremely fine nanopowders.
- It is an economic and facile technique to produce nanosized materials.
- It is a top down approach of nanoparticle synthesis which includes mechanical breakdown of large substance into smaller one.
- It is a ball milling process where a powder mixture is placed in the ball mill is was exposed to a high energy collision with a bullet.

4.4.2 STEPS IN BALL MILLING METHOD:

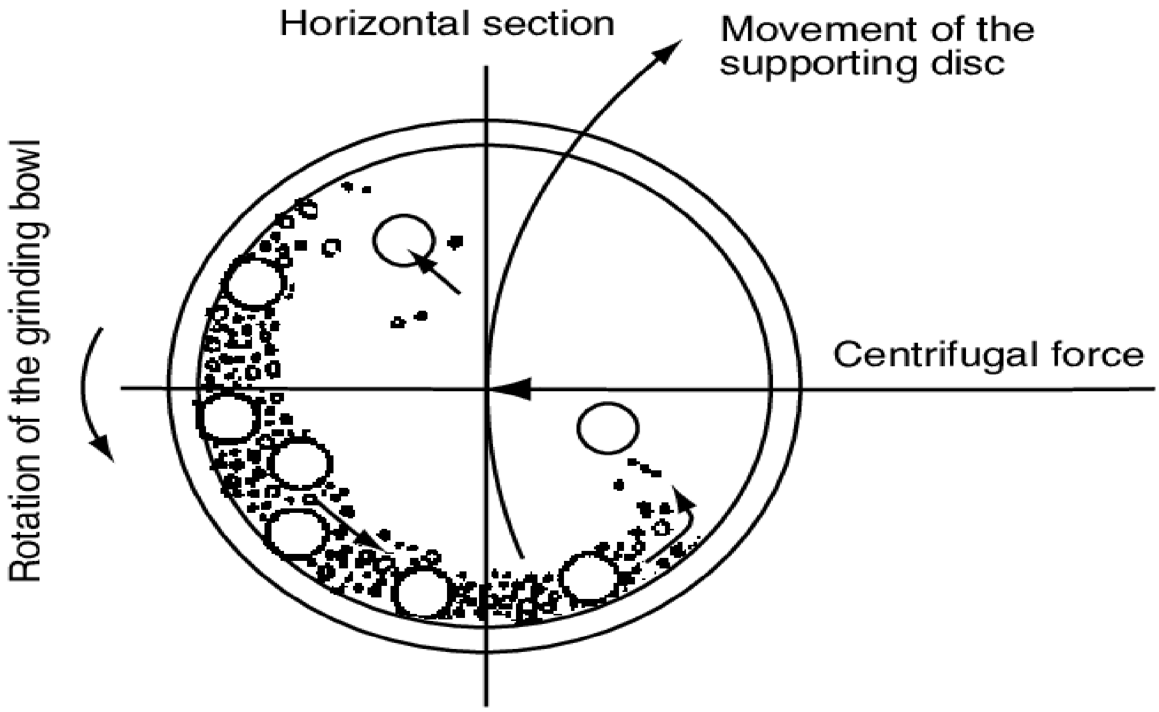

Fig.4.5 Ball milling method

- The ball milling method contains balls and a mill chamber. A ball mill contains a stainless steel container and many small ball made up of iron, hardness steel, tungsten carbide or silicon carbide are made to rotate inside a mill(drum).
- The powder of a material is taken in the steel container. This powder is nano-sized using ball mill technology. A magnet is placed on the outside of the hopper to apply a tensile force to the material, which increases the grinding energy as the grinding hopper or chamber rotates the metal balls.
- The ball to material mass ratio is maintained at 2 ratio.
- These silicon carbide balls provide a very large amount of energy to the material powder, which is then crushed.
- Since ball mill grinding is a mechanical process, all structural and chemical changes are generated by mechanical energy.

4.4.3 ADVANTAGES OF BALL MILLING METHOD:

Ball milling produces very fine powder (particle size less than or equal to 10 microns). Since it can be used in a completely closed form, it is suitable for crushing toxic substances. It has a wide application. It can be used for continuous operation and also used in milling highly abrasive materials.

4.4.4 DISADVANTAGES OF BALL MILLING METHOD:

Ball milling is bulky size; running a strong vibration and noise, there must be a solid foundation. It has low efficiency, energy consumption is relatively large; and it grinding the friction loss and a great body, and will stain products. It is a common material to crush hard materials.

CHAPTER 5

RESUT AND DISCUSSION

5.1 PREPARATION OF Sn Te0.5 Se0.5 MATERIALS:

The SnTe0.5 Se0.5 material were synthesized by high energy ball milling technique at room temperature. For synthesizing SnTe0.5 Se0.5, first Sn(Tin), Tellurium(Te) and Selenium(Se) materials were weighted in the ratio of 1:0.5:0.5 respectively. Then the apparatus was cleaned and the material were load and set to process. The sample have processed in the high energy ball milling for 5 hours using tungsten carbide vial with balls. Within every 30 minutes, the apparatus is set free and the inner sides of the vial must be cleaned inorder to remove the materials which have been sticked at the sides to make the material mix properly. Here the 5 hours of sample processing in tungsten carbide vial is equal to the 10 hours of sample processing in stainless steel vial. So tungsten carbide vials were preferred in this process. After 5 hours of processing in ball milling technique the SnTe0.5 Se0.5 have became a fine powder. Then the material was made as a pellet using the pelletizer for the further application of its thermoelectric properties.

Fig. 5.1 Ball milling equipment

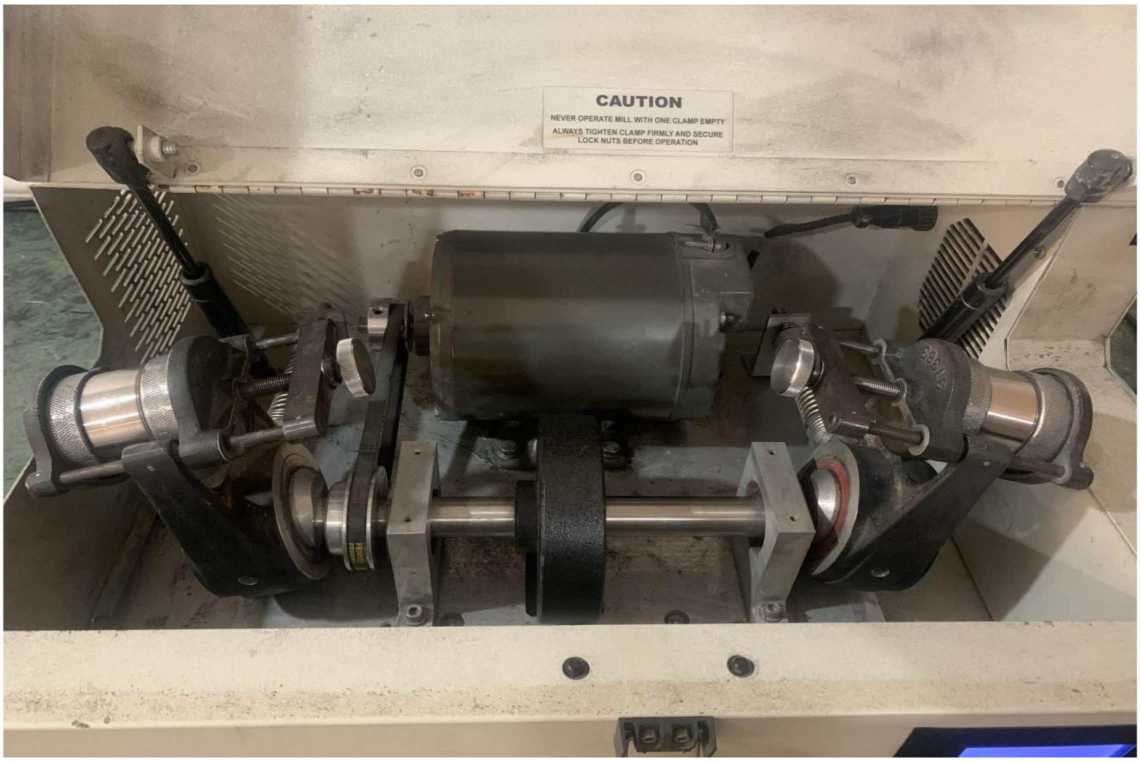

Fig. 5.2 Inside image of the ball milling apparatus

The below image was taken during the process of cleaning the vial at the beginning. In order to remove the other impurities sand was used.

Fig.5.3 Cleaning process of vial

Fig.5.4 Final SnTe0.5 Se0.5 material after ball milling

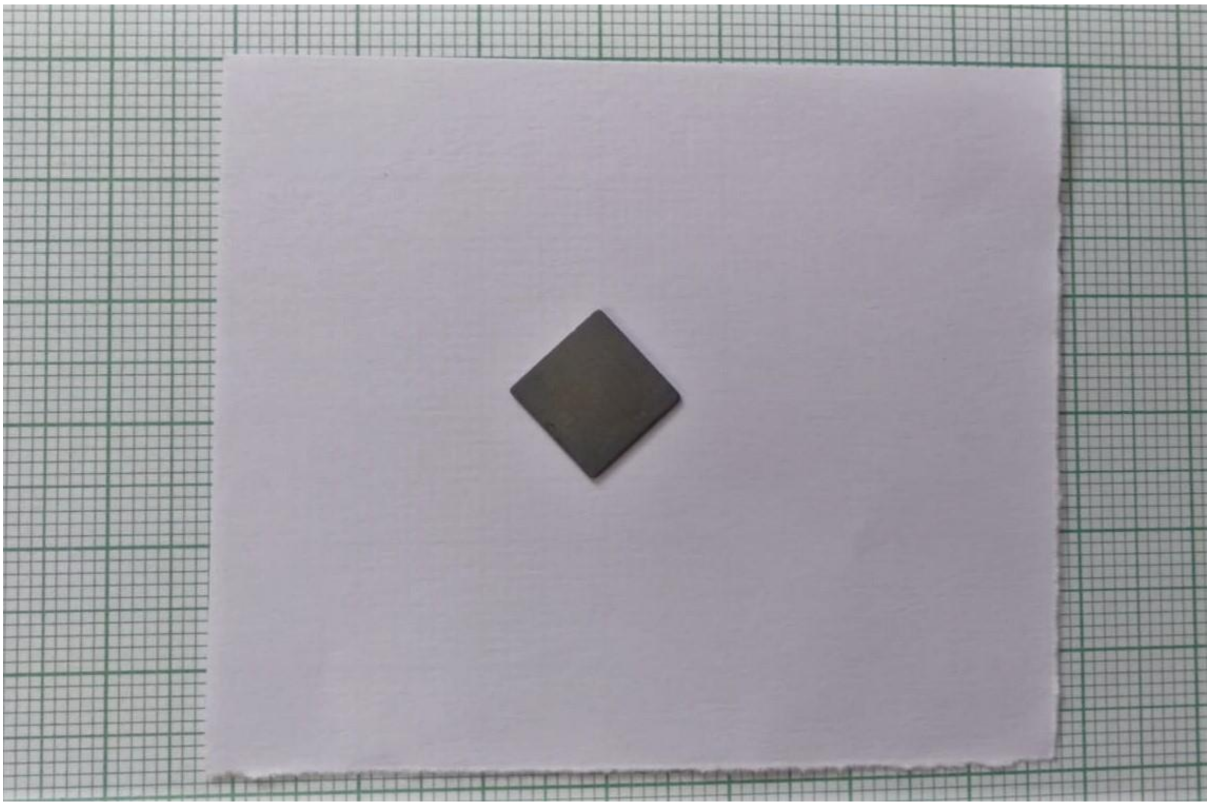

Fig 5.5 pellet

Pelletization is the process of compressing or shaping a material into pellets. A variety of materials are pelleted, including chemicals, iron ore, compound animal feeds, and plastics.

5.2 CHARACTERIZATION

5.2.1 Scanning electron microscopy (SEM) analysis:

Scanning electron microscope (SEM) is one of the most widely used techniques used in characterization of nano materials and nanostructures. The signals that derive from electron-powder materials interactions reveal information about the sample including surface morphology chemical composition of the sample. Scanning microscopy (SEM) is another technique where only milligram quantities of fabric could also be used to determine particle size, shape, and texture. In SEM a fine beam of electrons scan across the prepared sample during a series of parallel tracks. The electrons interact with the sample, and produce several different signals which may be detected and displayed on the screen of a beam tube. Particles smaller than 1 nm are often viewed, and since the depth of focus is such a lot greater than that of the light microscope, information on surface texture are often generated. SEM requires more time-consuming sample preparation than optical microscopy, and can't distinguish between crystalline and non-crystalline materials. However, when SEM is employed with other techniques like laser diffraction, it can provide valuable additional information on particle texture, which can help to elucidate agglomeration or flow problems.

The morphology of the SeTeSn composites was assessed based on SEM images. Figure 5.6-5.10 presents SEM images of composites surfaces at a magnification of 10000x. SEM images show that the surface structures of the “skins” of both membranes are significantly different.

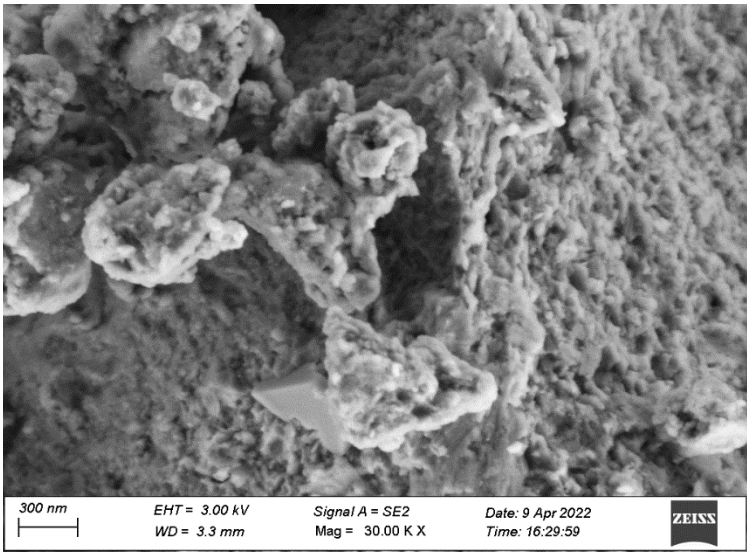

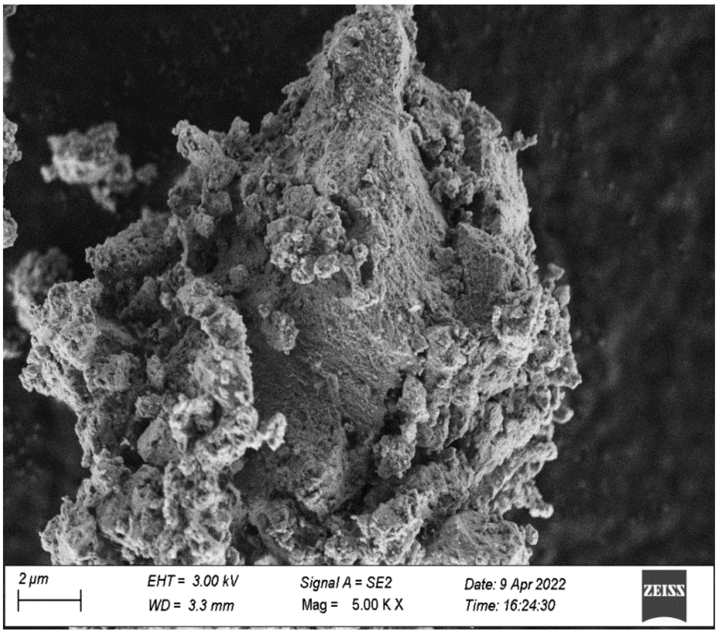

Fig.5.6-5.7 Scanning Electron Microscopy images of SeTeSn composites

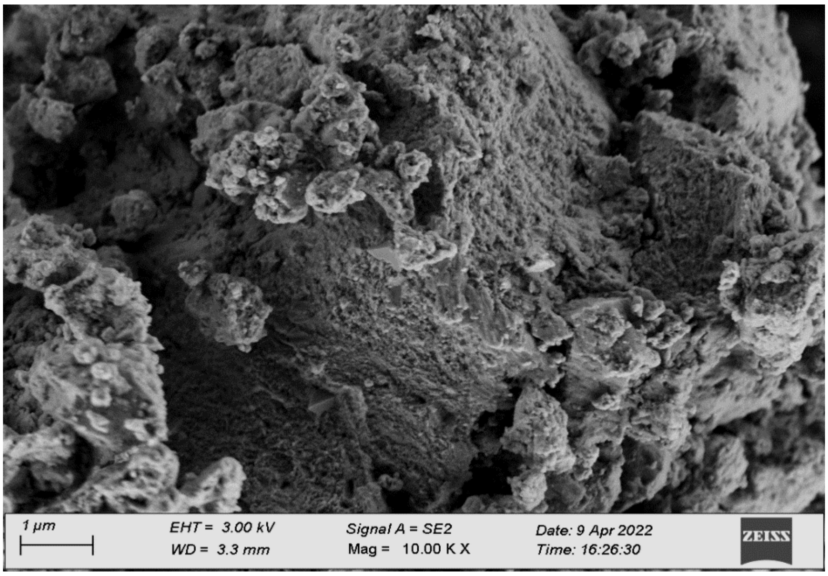

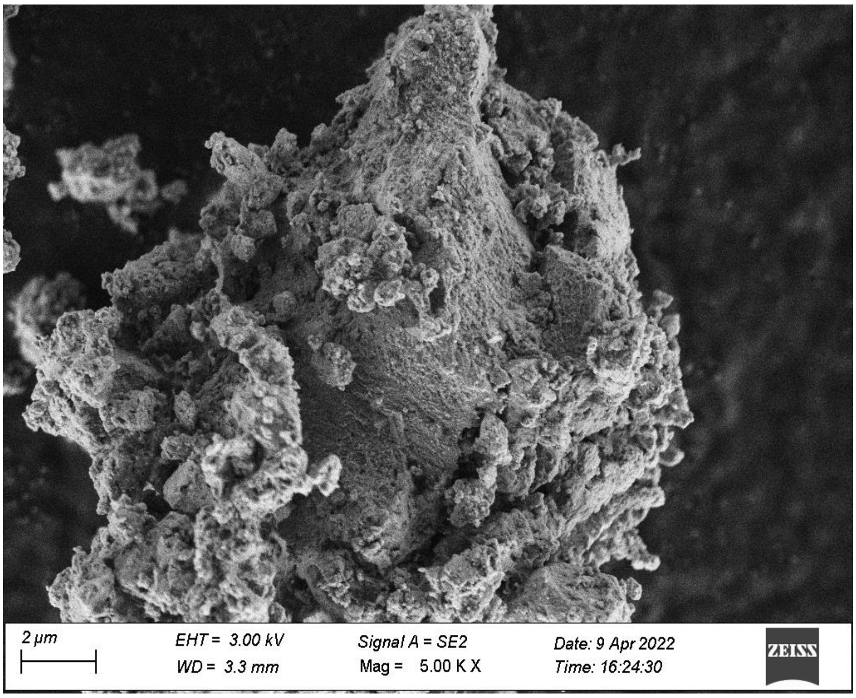

Fig.5.8-5.9 Scanning Electron Microscopy images of SeTeSn composites

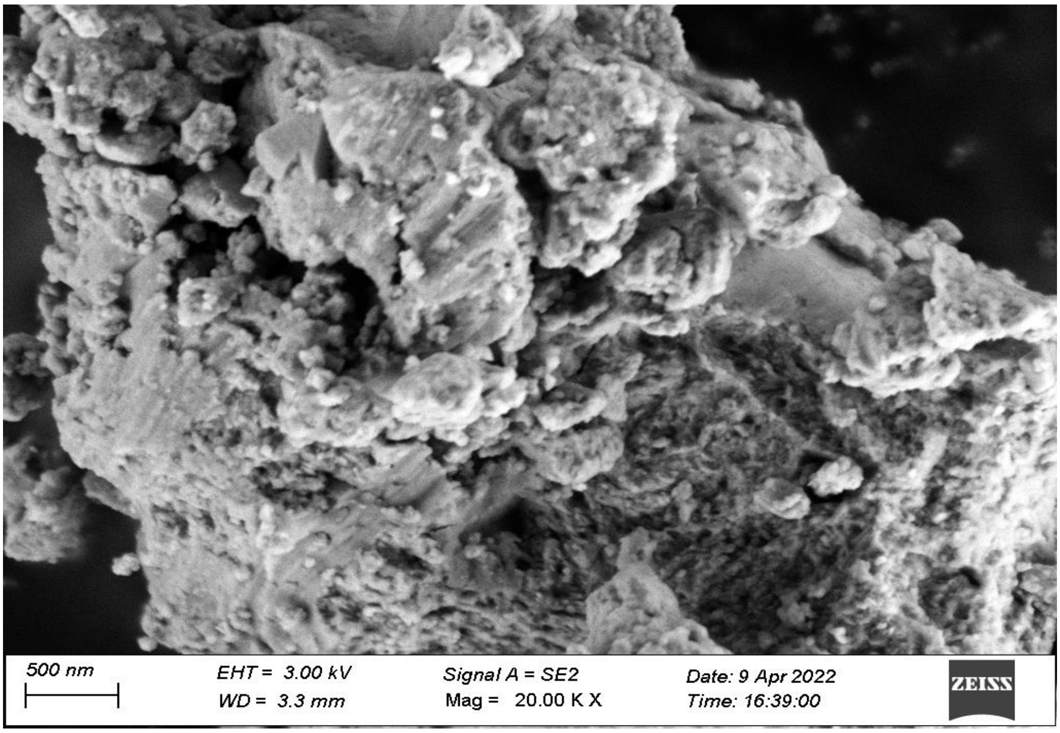

Fig.5.10 Scanning Electron Microscopy images of SeTeSn composites

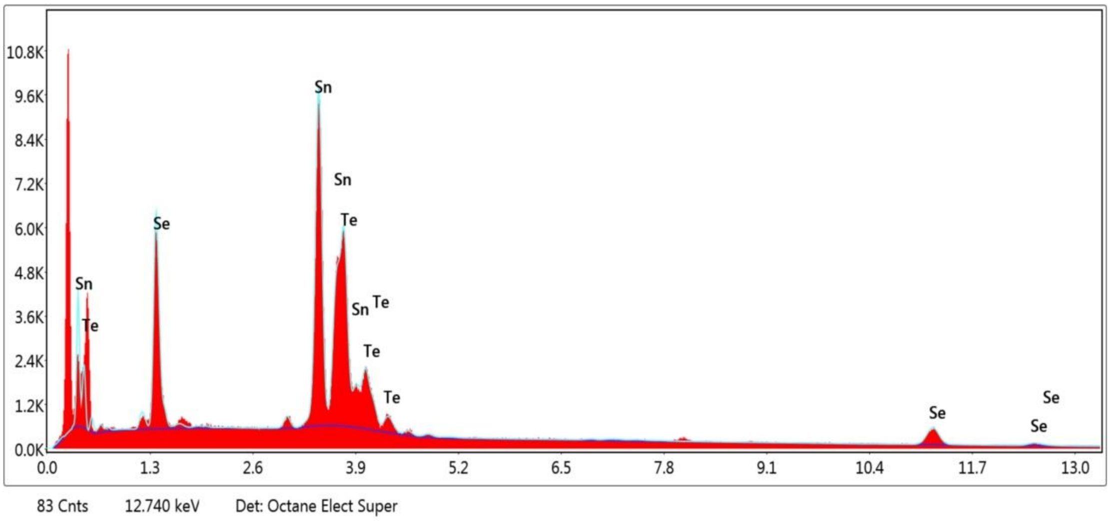

Fig.5.11 Edx analysis of SeTeSn composites

EDAX analysis of SeTeSn composites by EDAX

Energy Dispersive X-Ray Analysis (EDX), mentioned as EDS or EDAX, is an x-ray technique used to identify the basic composition of materials .Applications include materials and merchandise research, troubleshooting, deformulation, and more. EDX systems are attachments to microscopy instruments (Scanning electron microscopy (SEM) or Transmission electron microscopy (TEM)) instruments where the imaging capability of the microscope identifies the specimen of interest. The data generated by EDX analysis contains spectra showing peaks corresponding to the elements making up truth composition of the sample being analyzed. Elemental mapping of a sample and image analysis also are possible

Table.5.1 Composition and % of element present in the sample by EDX analysis

Element	Weight %	Atomic %	series	Error%
Sn	51.04	47.54	L	2.02
Te	30.13	26.11	L	3.71
Se	18.83	26.38	K	6.81

The Energy Dispersive X-ray (EDX) analysis is involved in different biomedical fields of study due to its high sensitivity in detecting the different elements in tissues. In fact, EDAX technique is made particularly useful in the study of drugs delivery in which the EDAX is an important tool in order to detect nanoparticles. EDAX technique is also used in the study of environmental pollution.

EDAX were used to find the elemental composition in the raction mixture. The EDAX analysis of SnTeSe composites was done by the SEM machine. The EDAX normally reveals the presence of phases. By using EDAX, we have attempted to correlate the elemental composition measured across a particle to representatives of the different classes of elements identified. The typical results are summarized.(Fig.5.1). EDAX of sample revealed the presence of pure Se,Sn, Te was the major constituents element. The EDAX reading proved that the required phase of given sample.

5.2.2 X-Ray Diffraction (XRD) analysis

X-Ray Diffraction may be a technique employed to work out the underlying crystal structure of a material; it enables verification of the crystallinity and structure of a sample but gives no information of a chemical nature. Fitting X-ray diffraction patterns can allow calculation of the fabric lattice parameters, the orientation of a crystal (or grain), stress in crystalline regions, and secondary phases within the sample. It is generally a bulk characterization technique and produces a mean diffraction pattern for the area measured. X-Ray Diffraction may be a nondestructive technique which may be conducted at temperature and pressure.

X-Ray Diffraction may be a technique used to determine the character of the materials as crystalline or amorphous. It'll define the quantification of cementitious materials.The X-Ray Diffraction analysis is completed with an X-ray source of Cu Kα radiation (λ = 1.5406 Å). It’ll analyze and identify the unknown crystalline compounds by Brag Brentano method. the various parameters like scan step size, collection time, range, X-ray tube voltage and current should be fixed supported the specimen's requirement analysis.

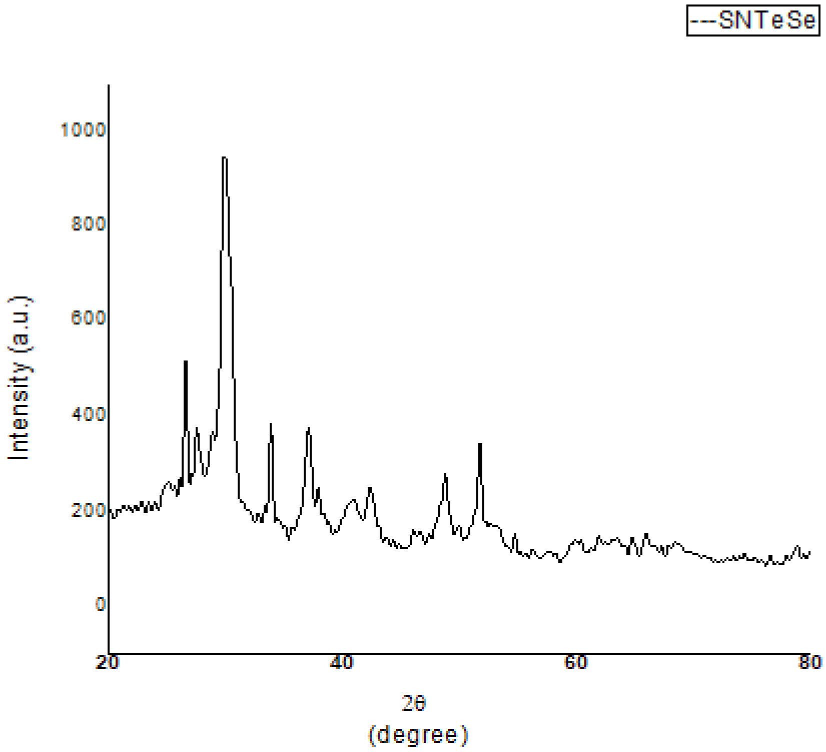

Fig.5.12 XRD analysis of SnTeSe composites

Samples, for X-ray diffraction analysis, were prepared as per the standard practice. Fig.5.12 show an Xray diffraction (XRD) pattern taken for SnTeSe composites to verify its quality. The X-ray diffraction pattern in Fig.5.12 shows that three highest intensity peaks at 33°,35° ,38°,44°,49° & 52° are distinctly visible for Sn,Te, and Se. This is believed to be due to good quality as well as due to the preferred orientation in the powder samples.

5.2.3 Measurement of the electrical resistivity and Hall coefficient at high temperatures

The electrical resistivity and Hall coefficient are important materials properties. They play an important role in any field of research concerned with the electronic transport properties of materials such as semiconductors and metals. From the Hall coefficient, the charge carrier concentration can be directly calculated. By simultaneous measurement of the resistivity, the carrier mobility can also be inferred. The temperature dependence and magnitude of the carrier mobility makes it possible to extract information about the scattering mechanisms.1 This cannot be done with separated measurements of the resistivity and Hall coefficient.

Hall effect

The conductivity, σ, of a sample at room temperature will be determined. The Hall Effect voltage, VH, and Hall coefficient, RH, for the same sample will be measured using a magnetic field. These measurements will enable the student to determine: the type (n or p) and doping density of the sample as well as the majority carrier's "Hall mobility."

The model Hall effect system consists of a uniform slab of electrically conducting material through which a uniform current density flows in the presence of a perpendicular applied magnetic field. The Lorentz force deflects moving charge carriers to one side of the sample and generates an electric field perpendicular to both the current density and the applied magnetic field. The Hall coefficient is the ratio of the perpendicular electric field to the product of current density and magnetic field, while the resistivity is the ratio of the parallel electric field to the current density.

Inspired by the free electron model, the Hall carrier concentration can be defined from the Hall coefficient as $nH = -1/eRH$ for electrons or $pH = 1/eRH$ for holes where e is the electron charge. For materials with more complex band structures, nH simply becomes a measure of the Hall coefficient in units related to carrier concentration that can be negative or positive. Together with the resistivity, the Hall mobility can also be defined as $\mu H = 1/nH\ e\rho$ or $\mu H = 1/pHe\rho$ for electrons and holes, respectively. For complicated systems, we define $\mu H = 1/nHe\rho = RH/\rho$ as simply a measure of the Hall effect in units of mobility that would be negative for electrons and positive for holes. For materials where a simple single band model does not apply, the results should be used with care since they can be quite far from the real charge carrier concentrations and mobilities. This is frequently apparent when more than one carrier type is present. In this case, the Hall voltages of the two species partially cancel leading to low values of RH and μH or high nH where the magnitude and sign of the values depend in a complicated way on the transport parameters of the individual species

The measured resistivity is not affected much if the temperature changes slightly during the measurement; however, fine features in the resistivity versus temperature curve might be lost. Both ac and dc measurements can be used with the method described here. Alternating current measurements are often considered to give more precise measurements but are also harder to implement as shielding and capacitance considerations are different. An ac magnetic field with an ac test current through the sample can also be used for measurement of the Hall effect.

Table.5.2 Conductivity, sheet conductivity, sheet resistance of $SnTe_{0.5}Se_{0.5}$ at initial current 1.0mA

No	Current [mA]	Bulk Conductivity [S/m] x10^{18}	Sheet Conductivity [S/m] x10^{17}	Sheet Resistance [Ωm]x10^{2}	Resistivity [Ωm]	Conductivity [S/m] X10^{-1}	BC [mV]x10^{1}	AC [mV]
1	1.00	-1.69	-84.3	1.12	5.56	1.80	-2.87	8.13
2	1.00	4.27	2.13	1.12	5.56	1.80	-2.87	8.08
3	1.00	35.6	17.8	1.12	5.57	1.79	-2.87	8.06
4	1.00	1.16	57.9	1.13	5.58	1.79	-2.87	8.02
5	1.00	-2.33	-1.17	1.13	5.59	1.79	-2.88	8.05

Table.5.3 Magnetic resistance, mobility, average hall co efficient, AC, BD & AB Hall data of $SnTe_{0.5}Se_{0.5}$ at initial current 1.0mA

No	Current (mA)	Magneto Resistance[T^{-1}] x10^{-2}	Mobility [$m^2/(V.s)$] x10^{-1}	Average Hall coefficient [m^3/C]	AC Hall [mV]	BD Hall [mV]	Ratio V/H x10^{-1}	AB [mV] x10^{1}
1	1.00	3.38	6.66	-3.70	-34.8	27.4	7.20	-2.07
2	1.00	2.00	2.63	1.46	-8.49	11.4	7.21	-2.07
3	1.00	5.34	0.314	17.5	25.3	9.78	7.21	-2.08
4	1.00	7.71	9.65	5.39	-30.4	41.2	7.22	-2.08
5	1.00	6.88	4.79	-2.68	-45.1	39.8	7.23	-2.08

Table.5.4 Different voltage characteristics of SnTe$_{0.5}$Se$_{0.5}$ at initial current 1.0mA by hall effect measurements.

S.No	-AB[mV] x10^{1}	-BC[mV] x10^{1}	-AC[mV]	CD[mV] x10^{1}	DA [mV] x10^{1}	BD [mV]	-CD [mV] x10^{1}	-DA [mV] x10^{1}	-BD [mV]
1	2.08	2.88	-8.01	-2.06	-2.88	8.11	2.08	2.89	-7.97
2	2.08	2.89	-7.96	-2.07	-2.87	8.06	2.08	2.89	-7.94
3	2.09	2.89	-8.00	-2.07	-2.88	8.09	2.08	2.89	-7.99
4	2.09	2.89	-7.98	-2.08	-2.88	8.07	2.09	2.90	-7.96
5	2.10	2.89	-7.92	-2.08	-2.88	8.02	2.10	2.90	-7.92

Table.5.5 Different voltage characteristics of SnTe$_{0.5}$Se$_{0.5}$ at initial current 1.0mA by hall effect measurements.

S.No	Initial current (ma)	MAC[mV] (N->S)	M-AC[mV] (N->S)	MBD[mV] (N->S)	M-BD[mV] (N->S)	-MAC[mV] (S->N)	-M-AC[mV] (S->N)	-MBD[mV] (S->N)	-M-BD[mV] (S->N)
1	1.00	8.09	-7.95	8.08	-7.93	8.16	-8.03	8.13	-7.99
2	1.00	8.06	-7.92	8.03	-7.90	8.07	-7.95	8.06	-7.92
3	1.00	8.11	-7.95	8.10	-7.92	8.03	-7.92	8.14	-7.92
4	1.00	8.10	-7.99	8.13	-7.97	8.13	-8.09	8.25	-8.03
5	1.00	8.06	-7.92	8.06	-7.94	8.12	-8.06	8.19	-7.99

Table.5.6 Conductivity, sheet conductivity, sheet resistance of $SnTe_{0.5}Se_{0.5}$ at initial current 1μA

No	Current[μA]	Bulk Conductivity [S/m] x10^{16}	Sheet Conductivity [S/m] x10^{15}	Sheet Resistance [Ωm] x10^{2}	Resistivity [Ωm]	Conductivity [S/m]
1	1.00	0.27	0.133	1.09	3.04E+00	3.29E-01
2	1.00	60.3	30.1	1.08	1.54E+01	6.50E-02
3	1.00	3.73	1.87	1.08	2.26E+01	4.43E-02
4	1.00	-1.17	-58.4	1.10	8.44E+03	1.18E-04
5	1.00	-1.62	-81.1	1.07	2.48E+03	4.03E-04
6	1.00	-2.94	-1.47	1.08	4.01E+06	2.50E-07
7	1.00	3.37	1.69	1.09	4.07E+05	2.46E-06
8	1.00	2.18	1.09	1.09	2.89E+02	3.46E-03
9	1.00	7.59	3.80	1.08	1.99E+02	5.03E-03
10	1.00	-3.81	-1.90	1.10	1.11E+02	9.02E-03

Table.5.7 Magnetic resistance, mobility, average hall co efficient , AC , BD & AB Hall data of $SnTe_{0.5}Se_{0.5}$ at initial current 1μA

NO	Magneto Resistivity [T^{-1}]	Mobility [$m^2/(V.s)$]	Average Hall coefficient [m^3/C] x10^2	AC Hall [mV] x10^2	BD Hall [mV] x10^2	Ratio V/H x10^{-1}	AB[mV] x10^{-3}	BC[mV] x10^{-2}	AC[mV] x10^{-2}
1	3.71	7.72E+00	23.4	1.67	-1.20	7.12	2.62	-1.75	2.96
2	1.55	6.74E+01	0.11	0.193	1.44	6.94	3.05	-1.60	2.87
3	1.74	7.42E+00	1.67	2.07	1.27	7.16	3.35	-1.66	2.88
4	1.02	6.33E-02	-5.35	-2.24	-8.45	7.23	4.40	-1.44	3.06
5	1.56	1.55E-01	-3.85	-4.81	-2.89	7.26	4.35	-1.47	2.95
6	3.63	5.30E-05	-2.12	-1.29	-2.96	7.04	5.02	-1.50	2.86
7	1.80	4.55E-04	1.85	-28.9	3.99	7.10	5.36	-1.49	2.87
8	1.33	9.93E-01	2.87	22.8	5.51	7.27	5.98	-1.38	3.05
9	2.48	4.13E-01	82.2	1.39	25.4	7.14	6.21	-1.40	3.03
10	1.24	1.48E+00	-1.64	1.76	-5.04	7.11	6.84	-1.48	3.01

Table.5.8 Different voltage characteristics of $SnTe_{0.5}Se_{0.5}$ at initial current 1.0μA by hall effect measurements

NO	-AB[mV] $x10^{-2}$	-BC[mV] $x10^{-2}$	-AC[mV] $X10^{-2}$	CD[mV] $X10^{-3}$	DA[mV] $x10^{-2}$	BD[mV] $X10^{-2}$	-CD[mV] $X10^{-2}$	-DA[mV] $X10^{-3}$	-BD[mV] $X10^{-3}$
1	4.17	3.85	1.35	-10.5	-2.36	1.83	3.06	3.30	1.14
2	4.21	3.94	1.35	-9.88	-2.13	1.80	2.93	3.61	3.38
3	4.26	3.94	1.29	-9.10	-1.88	1.88	3.14	3.67	2.99
4	4.48	4.23	1.47	-9.12	-1.73	1.85	3.23	3.92	3.70
5	4.43	4.07	1.31	-9.24	-1.58	1.83	3.02	3.82	2.60
6	4.43	4.04	1.24	-9.07	-1.80	1.77	3.06	3.88	2.33
7	4.43	3.99	1.33	-9.72	-1.76	1.85	3.14	4.04	3.08
8	4.68	4.27	1.60	-6.47	-1.29	2.01	3.36	4.18	3.68
9	4.66	4.24	1.49	-7.02	-1.35	1.93	3.20	4.12	2.24
10	4.64	4.17	1.32	-8.04	-1.55	1.83	3.32	4.16	3.45

Table.5.9 Different voltage characteristics of $SnTe_{0.5}Se_{0.5}$ at initial current 1.0μA by hall effect measurements

NO	MAC[mV] (N->S)$x10^{-2}$	M-AC[mV] (N->S)$x10^{-2}$	MBD[mV] (N->S)$x10^{-2}$	M-BD[mV] (N->S)$x10^{-3}$	-MAC[mV] (S->N) $x10^{-2}$	-M-AC[mV] (S->N) $x10^{-2}$	-MBD[mV] (S->N)$x10^{-2}$	-M-BD[mV] (S->N) $x10^{-3}$
1	2.83	1.21	1.68	1.02	4.04	2.48	1.90	3.71
2	3.05	1.28	1.89	3.16	2.43	1.50	2.03	3.93
3	3.11	1.50	1.87	2.84	3.22	1.70	2.01	3.62
4	3.02	1.49	1.94	3.66	3.27	1.64	1.73	5.21
5	2.96	1.44	2.02	3.70	3.25	1.52	1.95	4.32
6	2.88	1.34	1.77	1.52	2.59	0.995	2.84	13.5
7	3.02	1.45	1.99	3.50	3.21	1.63	2.16	3.45
8	3.15	1.50	1.96	5.37	2.87	1.23	2.07	4.07
9	2.92	1.27	1.71	1.25	2.78	1.19	2.27	6.75
10	3.00	1.42	2.03	2.83	2.86	1.35	2.07	5.44

Table.5.10 Conductivity, sheet conductivity, sheet resistance of $SnTe_{0.5}Se_{0.5}$ at initial current 2 mA

No	Current[mA]	Bulk Conductivity [S/m] x10^{17}	Sheet Conductivity [S/m] x10^{16}	Sheet Resistance [Ωm] x10^{2}	Resistivity [Ωm]	Conductivity [S/m] x10^{-1}
1	2.00	4.22	2.11	1.13	5.62	1.78
2	4.00	-0.122	-6.08	1.13	5.61	1.78
3	6.00	2.12	1.06	1.13	5.61	1.78
4	8.00	1.86	92.8	1.13	5.61	1.78
5	1.00	2.14	1.07	1.13	5.60	1.79
6	1.20	-2.01	-1.01	1.13	5.59	1.79
7	1.40	-8.61	-4.31	1.13	5.57	1.79
8	1.60	-92.0	-46.0	1.12	5.55	1.80
9	1.80	1.85	92.4	1.12	5.53	1.81
10	2.00	-3.25	-1.62	1.11	5.50	1.82

Table.5.11 Magnetic resistance, mobility, average hall co efficient , AC , BD & AB Hall data of $SnTe_{0.5}Se_{0.5}$ at initial current 2 mA

NO	Magneto Resistivity [T^{-1}] X10^{-2}	Mobility [$m^2/(V.s)$]	Average Hall coefficient [m^3/C]	AC Hall [mV]	BD Hall [mV]	Ratio V/H x10^{-1}	AB[mV] x10^2	BC[mV] x10^2	AC[mV] x10^2
1	7.20	2.63	0.148	-0.254	0.550	7.21	-41.9	-57.9	16.2
2	6.47	91.4	-5.130	-0.163	6.08	7.19	-83.7	-1.16	32.7
3	6.14	5.24	0.294	-0.138	0.727	7.19	-1.26	-1.74	48.5
4	0.173	6.00	0.336	-0.125	0.798	7.17	-1.68	-2.33	64.9
5	0.229	5.22	0.292	6.95	0.515	7.10	-2.09	-2.90	82.4
6	0.119	5.54	-0.310	-0.971	0.351	7.08	-2.50	-3.49	1.02
7	0.108	1.30	-7.250	-0.0104	0.895	7.04	-2.90	-4.07	1.21
8	0.215	0.122	-0.679	-0.0226	0.898	7.05	-3.30	-4.66	1.32
9	0.297	6.11	0.338	0.423	0.253	7.03	-3.71	-5.21	1.41
10	0.157	3.49	-0.192	-0.481	9.67	7.06	-4.12	-5.76	1.65

Table.5.12 Different voltage characteristics of $SnTe_{0.5}Se_{0.5}$ at initial current 2 mA by hall effect measurements.

NO	-AB[mV] x10^2	-BC[mV] x10^2	-AC[mV] x10^2	CD[mV] x10^2	DA[mV] x10^2	BD[mV] x10^2	-CD[mV] x10^2	-DA[mV] x10^2	-BD[mV] x10^2
1	42.1	58.1	-16.0	-41.8	-58.2	16.5	41.9	58.3	-16.3
2	83.9	1.17	-32.7	-83.3	-1.16	32.6	83.7	1.16	-32.2
3	1.26	1.74	-49.2	-1.25	-1.75	49.3	1.25	1.75	-48.1
4	1.67	2.32	-66.1	-1.66	-2.33	64.9	1.67	2.33	-64.9
5	2.08	2.91	-83.2	-2.05	-2.93	86.0	2.06	2.93	-83.8
6	2.49	3.49	-1.02	-2.46	-3.52	1.05	2.47	3.51	-1.01
7	2.89	4.08	-1.23	-2.85	-4.09	1.22	2.86	4.10	-1.21
8	3.30	4.64	-1.42	-3.24	-4.67	1.38	3.27	4.62	-1.37
9	3.71	5.19	-1.62	-3.61	-5.24	1.55	3.62	5.22	-1.52
10	4.08	5.75	-1.73	-4.01	-5.79	1.74	4.02	5.70	-1.68

Table.5.13 Different voltage characteristics of SnTe $_{0.5}$Se $_{0.5}$ at initial current 2 mA by hall effect measurements.

S.NO	MAC[mV] (N->S) x10^2	M-AC[mV] (N->S) x10^2	MBD[mV] (N->S) x10^2	M-BD[mV] (N->S) x10^2	-MAC[mV] (S->N) x10^2	-M-AC[mV] (S->N) x10^2	-MBD[mV] (S->N) x10^2	-M-BD[mV] (S->N) x10^2
1	16.2	-16.0	16.7	-16.1	16.3	-16.1	16.7	-16.5
2	32.9	-32.6	32.9	-32.7	33.0	-32.8	33.3	-32.4
3	48.9	-49.1	48.9	-47.6	49.0	-49.3	49.5	-48.9
4	66.4	-65.8	67.3	-64.9	66.3	-66.3	68.3	-66.7
5	86.3	-85.9	85.5	-85.4	86.3	-85.6	86.9	-86.3
6	1.02	-1.02	1.03	-1.02	1.05	-1.04	1.04	-1.03
7	1.19	-1.22	1.22	-1.21	1.23	-1.24	1.24	-1.24
8	1.27	-1.34	1.35	-1.36	1.38	-1.39	1.40	-1.38
9	1.56	-1.57	1.55	-1.54	1.55	-1.56	1.56	-1.54
10	1.71	-1.73	1.74	-1.71	1.74	-1.74	1.75	-1.71

Table.5.14 Conductivity, sheet conductivity, sheet resistance of SnTe $_{0.5}$Se $_{0.5}$ at different current

No	Current[A]	Bulk Conductivity [S/m] x10^{17}	Sheet Conductivity [S/m] x10^{16}	Sheet Resistance[Ωm] x10^{2}	Resistivity [Ωm]	Conductivity [S/m] x10-1	Magneto Resistance [T^{-1}] x10^{-2}
1	1.00E-05	-6.93	-3.46	1.14	5.63	1.78	0.423
2	2.00E-05	-6.78	-3.39	1.14	5.65	1.77	0.162
3	3.00E-05	-0.151	-7.53	1.15	5.68	1.76	0.140
4	4.00E-05	2.20	1.10	1.14	5.66	1.77	4.83
5	5.00E-05	9.95	4.98	1.14	5.66	1.77	6.53
6	6.00E-05	5.54	2.77	1.14	5.67	1.77	0.118
7	7.00E-05	7.56	3.78	1.15	5.67	1.76	7.71
8	8.00E-05	-0.972	-0.486	1.15	5.68	1.76	7.43
9	9.00E-05	0.248	0.124	1.15	5.68	1.76	5.92
10	1.00E-04	0.109	5.43	1.15	5.70	1.76	3.16

Table.5.15 Magnetic resistance, mobility, average hall co efficient , AC , BD & AB Hall data of $SnTe_{0.5}Se_{0.5}$ at different current

S.NO	Mobility [m^2 /(V. s)]	Average Hall coefficient	AC Hall[mV]	BD Hall [mV]	Ratio V/H x10^{-1}	AB[mV]	BC[mV]	AC[mV] x10^{-1}	-AB[mV]
1	1.60	-9.01	0.496	-0.676	7.13	-17.2	-27.7	1.19	24.4
2	1.63	-9.21	0.237	-0.421	7.13	-39.3	-57.2	1.96	44.4
3	73.0	-4.14	-0.250	0.167	7.07	-60.6	-86.8	2.76	65.0
4	5.01	0.284	0.422	0.146	7.11	-81.6	-1.14	3.64	86.2
5	1.11	6.27	6.07	6.47	7.12	-1.01	-1.44	4.45	1.09
6	1.99	0.113	-0.181	0.406	7.13	-1.22	-1.74	5.33	1.30
7	1.46	8.25	-0.325	0.490	7.12	-1.43	-2.03	6.18	1.51
8	11.3	-64.2	0.265	-0.278	7.09	-1.64	-2.34	7.11	1.72
9	44.3	2.51	0.405	-0.354	7.08	-1.85	-2.64	8.06	1.93
10	1.01	5.74	0.242	-0.127	7.06	-2.06	-2.94	9.11	2.14

Table.5.16 Different voltage characteristics of SnTe$_{0.5}$Se$_{0.5}$ at different current by hall effect measurements

S.NO	-BC[mV]	-AC[mV] x10^{-1}	CD[mV]	DA[mV]	BD[mV] x10^{-1}	-CD[mV]	-DA[mV]	-BD[mV] x10^{-1}	MAC[mV] (N->S) x10^{-1}
1	30.8	-49.0	-19.9	-28.3	92.1	21.9	30.2	-74.2	1.17
2	60.3	-1.43	-41.0	-58.1	1.82	42.8	59.6	-1.58	1.96
3	91.2	-2.30	-61.9	-87.5	2.68	64.0	90.5	-2.42	2.77
4	1.21	-3.22	-82.6	-1.15	3.58	85.2	1.21	-3.32	3.68
5	1.50	-4.01	-1.02	-1.45	4.40	1.08	1.50	-4.12	4.52
6	1.80	-4.86	-1.23	-1.74	5.23	1.29	1.80	-4.96	5.41
7	2.10	-5.71	-1.44	-2.04	6.12	1.50	2.09	-5.82	6.23
8	2.40	-6.69	-1.65	-2.34	7.05	1.71	2.40	-6.78	7.16
9	2.70	-7.59	-1.86	-2.65	7.95	1.92	2.69	-7.68	8.19
10	3.01	-8.53	-2.07	-2.96	9.04	2.13	3.00	-8.66	9.12

Table.5.17 Different voltage characteristics of $SnTe_{0.5}Se_{0.5}$ at different current by hall effect measurements.

S.NO	M-AC[mV] (N->S) x10^{-1}	MBD[mV] (N->S) x10^{-1}	M-BD[mV] (N->S) x10^{-1}	-MAC[mV] (S->N) x10^{-1}	-M-AC[mV] (S->N) x10^{-1}	-MBD[mV] (S->N) x10^{-1}	-M-BD[mV] (S->N) x10^{-1}
1	-53.9	95.2	-75.7	1.10	-59.3	93.5	-74.5
2	-1.46	1.84	-1.59	1.89	-1.51	1.84	-1.55
3	-2.36	2.71	-2.46	2.85	-2.31	2.75	-2.44
4	-3.22	3.58	-3.29	3.65	-3.18	3.61	-3.29
5	-4.04	4.42	-4.13	4.52	-4.02	4.45	-4.12
6	-4.89	5.32	-4.98	5.43	-4.92	5.37	-5.03
7	-5.74	6.14	-5.81	6.28	-5.79	6.19	-5.91
8	-6.74	7.19	-6.71	7.18	-6.63	7.05	-6.74
9	-7.54	8.02	-7.74	7.99	-7.59	7.96	-7.65
10	-8.53	9.05	-8.64	9.14	-8.40	9.01	-8.63

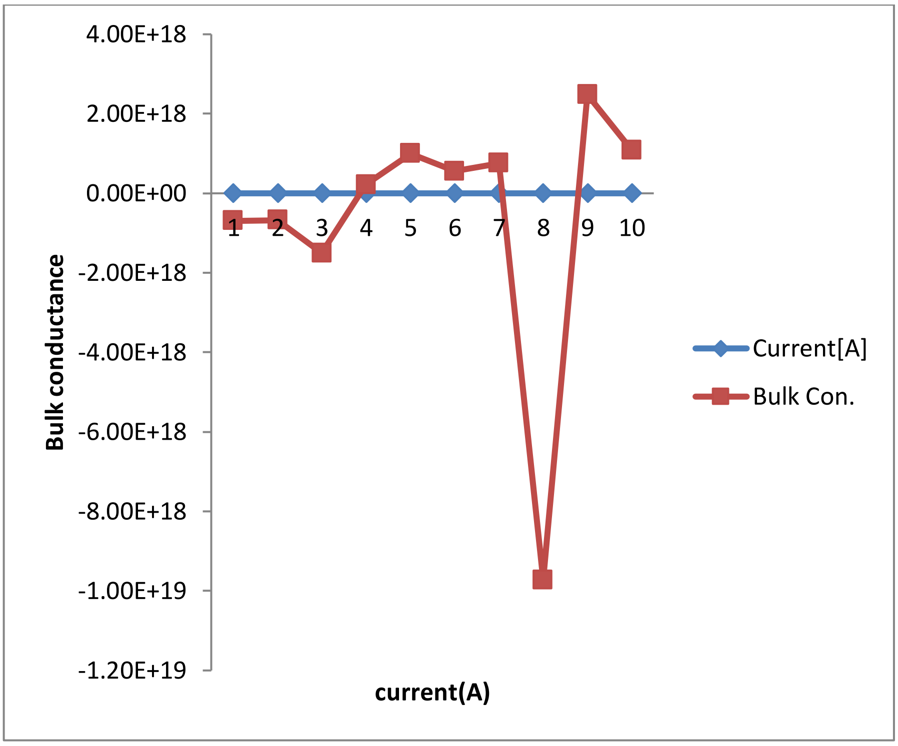

Fig.5.13 Variation of bulk conductance with different current of a composite by measurement of Hall volte

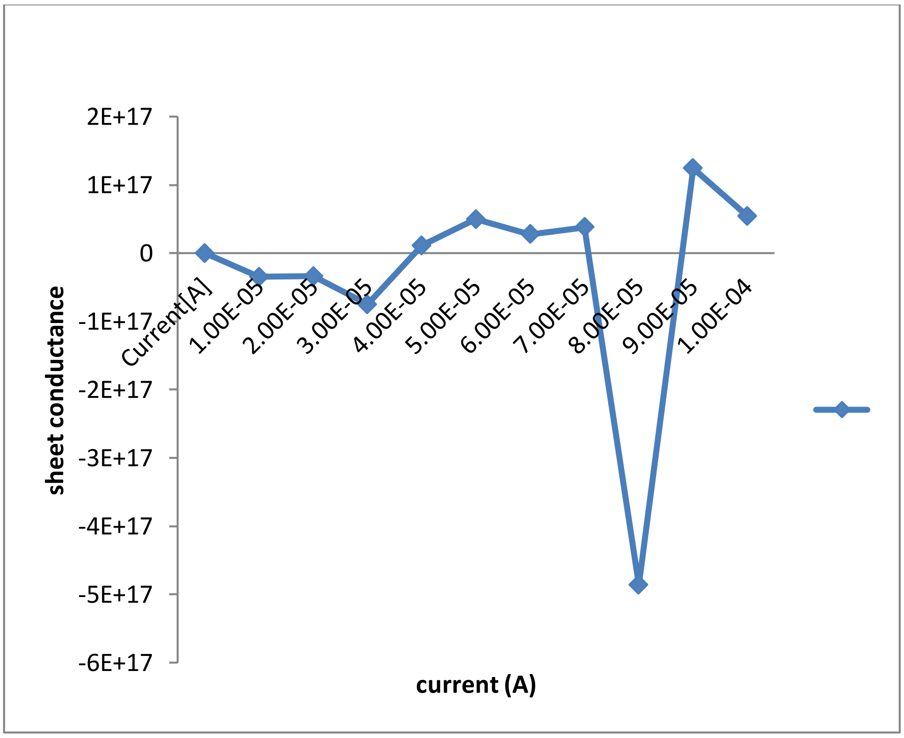

Fig.5.14 Variation of sheet conductance with different current of a composite by measurement of Hall volte

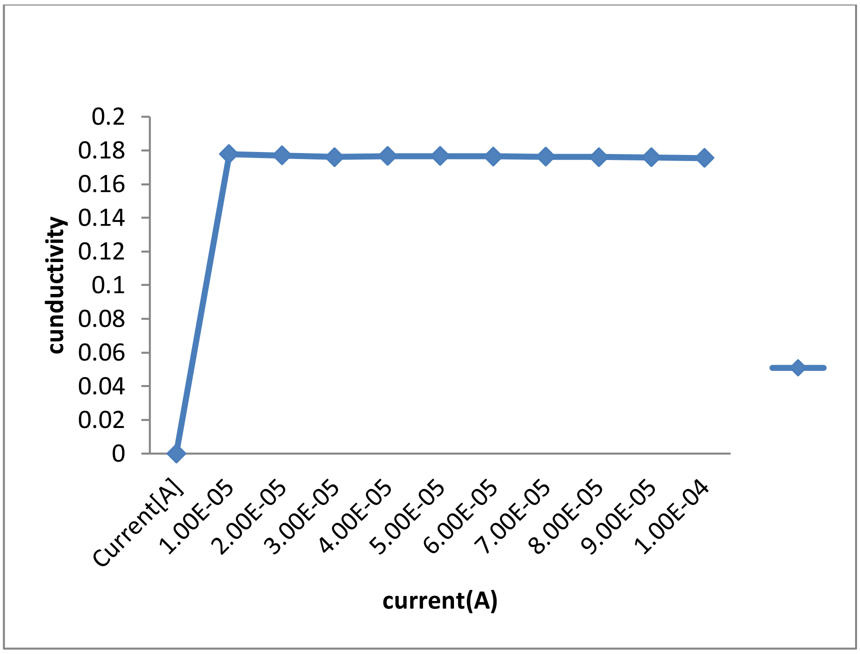

Fig.5.15 Variation of conductivity with different current of a composite by measurement of Hall volte

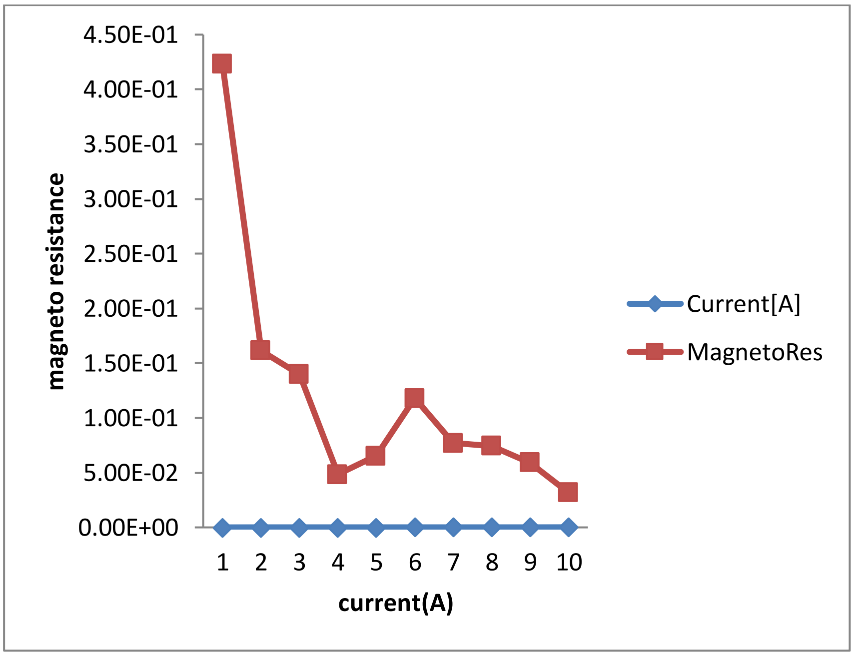

Fig.5.16 Variation of magneto resistance with different current of a composite by measurement of Hall volte.

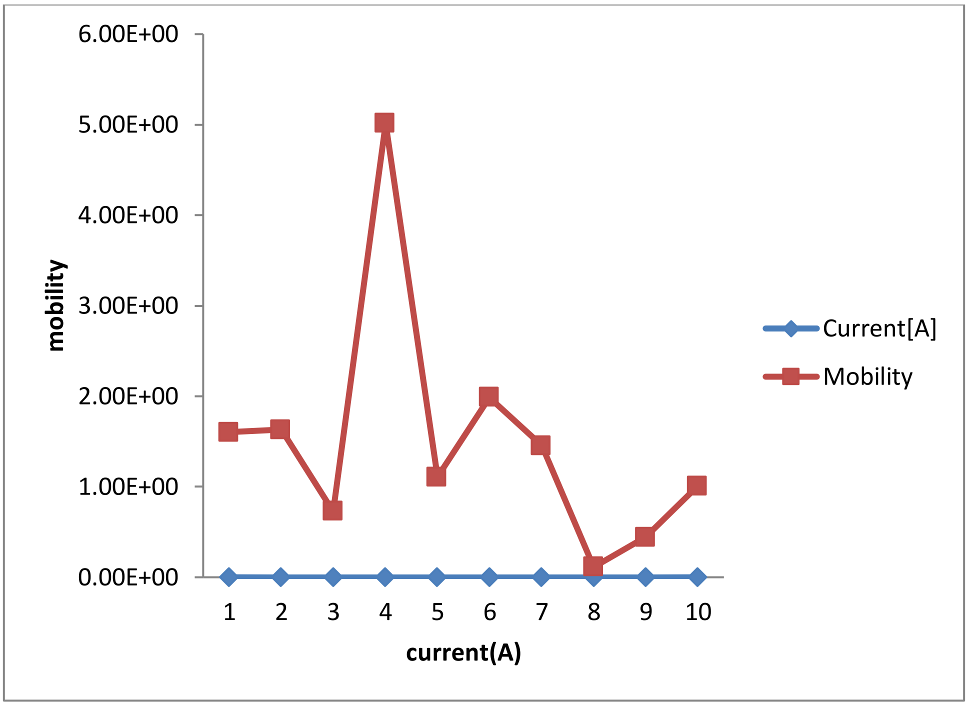

Fig.5.17 Variation of mobility with different current of a composite by measurement of Hall volte.

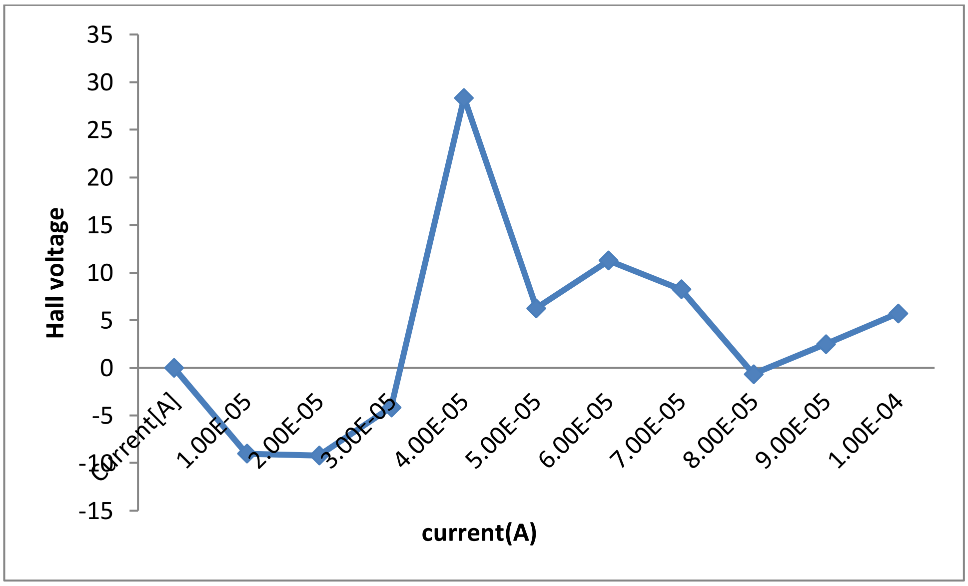

Fig.5.18 Variation of Hall voltage with different current of a composite by measurement of Hall volte

In this study, SnTeSe doped composites materials were prepared by ball milling method.

The basic physical principle underlying the Hall effect is the Lorentz force, which is a combination of two separate forces: the electric force and the magnetic force. When an electron moves along the electric field direction perpendicular to an applied magnetic field, it experiences a magnetic force $-q\mathbf{v} \times \mathbf{B}$ acting normal to both directions. The direction of this magnetic force can be determined by using the right hand rule convention. **Sheet resistance**, is a measure of resistance of thin films that are nominally uniform in thickness. It is commonly used to characterize materials made by semiconductor doping. The importance of the Hall effect is supported by the need to determine accurately carrier density, electrical resistivity, and the mobility of carriers in semiconductors. The Hall Effect provides a relatively simple method for doing this experiment.

The variation of the Hall voltage with current and its variation with magnetic field are shown, respectively, in Table. 5.2-5.17. The resistance of the sample changes when the magnetic field is turned on. These phenomena called magneto-resistance. It is due to the fact that the drift velocity of all carriers is not the same, with magnetic field on, the Hall voltage compensates exactly the Lorentz force for carriers with average velocity. Slower carriers will be over compensated and faster ones under compensated, resulting in trajectories that are not along the applied external field.

Conductivity, sheet conductivity was measured at 1ma, 1microamp, 2mA at room temperature. Sheet resistance, resistivity, conductivity and the value of BC and AC potential are measured as constant value. But the sheet conductivity and bulk conductivity are varied also it shows negative value. Similarly magneto resistance, mobility, average hall co efficient also measured at 1mA. Magneto resistance varied from 2 to 7.71(T^{-1}) . By using hall measurements, different voltage characteristics are also measured and all data given in Table. 5.2-5.17. Similarly Bulk conductivity, sheet conductivity, sheet resistance and resistivity are measured at **1μA.** In this case, bulk conductivity and sheet conductivity shows the negative value of composites when conductivity is gradually increased with applied potential. The same reflections are observed in the mobility, Hall co efficient and AC hall potential.

Similarly, Hall co-efficient parameters like conductivity, sheet conductivity, sheet resistance, resistivity of the material, magentoresistance and mobility are measured for a material $SnTe_{0.5}$ $Se_{0.5}$ with the initial current 2mA. The applied current is varied from 1mA to 2mA. The value of bulk conductivity and sheet conductivity are measured and the values are given in Table. 5.10 but only at particular current, the bulk conductivity and sheet conductivity shows the negative value. The negative bulk conductivity occurred at 4mA, 2mA, 1.60mA and 1.20mA. Similarly the negative sheet conductivity value occurred at the same applied current. The highest negative value appeared at 1.60mA. It is due to the sudden increase in charge carriers and high electron mobility of conducting materials. But the sheet resistance, conductivity and resistivity shows almost constant value.

The magneto resistivity and mobility data of the composite materials measured at 2mA are given in Table.5.11. The magneto resistivity varied from 0.108[T^{-1}] upto 7.20 [T^{-1}]. Similarly the mobility of charge carriers of a material are varied in randomly from 0.122 [m^2/V.s] upto maximum of 9.14[m^2/V.s]. The minimum mobility of a conductor appeared at 1.60mA and the highest mobility of charge carriers 9.14 [m^2/V.s] is appeared at 4mA. This variation is appeared due to the application of current and resistance of a material. The reflection of this data is also appeared in average hall co-efficient.

References:

1. Wang, L., Zheng, S., & Chen, H. (2016). Enhanced Electronic Transport Properties of Se-Doped SnTe1−xSex Nanoparticles by Microwave-Assisted Solvothermal Method. Journal of Electronic Materials, 46(5), 2847–2853.
2. Lu, W., He, T., Li, S., Zuo, X., Zheng, Y., Lou, X., … Tang, G. (2020). Thermoelectric performance of nanostructured In/Pb codoped SnTe with band convergence and resonant level via a green and facile hydrothermal method. Nanoscale.
3. Han, G., Zhang, R., Popuri, S., Greer, H., Reece, M., Bos, J.-W., … Gregory, D. (2017). Large-Scale Surfactant-Free Synthesis of p-Type SnTe Nanoparticles for Thermoelectric Applications. Materials, 10(3), 233.
4. Tan, L. P., Sun, T., Fan, S., Ramanujan, R. V., & Hng, H. H. (2014). Facile precipitation of two phase alloys in SnTe0.75Se0.25 with improved power factor. Journal of Alloys and Compounds, 587, 420–427.

5. Manjula, M., Muthumari, M., Krishnaveni, S., Kuznetsov, D., & Veluswamy, P. (2021). Influence of Ternary and Quaternary Inclusion on Bandgap Tuning of CaTe: Prediction of Potential Thermoelectric Materials. Journal of Electronic Materials, 50(4), 1759–1771.

6. He, J., & Tritt, T. M. (2017). Advances in thermoelectric materials research: Looking back and moving forward. Science, 357(6358),

7. Jaldurgam, F. F., Ahmad, Z., & Touati, F. (2021). Synthesis and Performance of Large-Scale Cost-Effective Environment-Friendly Nanostructured Thermoelectric Materials. Nanomaterials, 11(5), 1091.

8. He, J., Xu, J., Tan, X., Liu, G.-Q., Shao, H., Liu, Z., … Jiang, J. (2016). Synthesis of SnTe/AgSbSe 2 nanocomposite as a promising lead-free thermoelectric material. Journal of Materiomics, 2(2), 165–171.

9. Salavati-Niasari, M., Bazarganipour, M., Davar, F., & Fazl, A. A. (2010). Simple routes to synthesis and characterization of nanosized tin telluride compounds. Applied Surface Science, 257(3), 781–785.

10. Satyendra Singh[a)], Surasree Sadhukhan, Prakash Behera, and R. Venkatesh(2021). Structural, Morphological and Thermoelectric Studies of SnTe-Te Nanocomposite. AIP Conference Proceedings 2369(1):020072.

11. Wei, J., Yang, L., Ma, Z., Song, P., Zhang, M., Ma, J., … Wang, X. (2020). Review of current high-ZT thermoelectric materials. Journal of Materials Science. **55**, 12642–12704.

12. Sootsman, J. R., Chung, D. Y., & Kanatzidis, M. G. (2009). New and Old Concepts in Thermoelectric Materials. Angewandte Chemie International Edition, 48(46), 8616–8639.

13. Du, Y., Xu, J., Paul, B., & Eklund, P. (2018). Flexible thermoelectric materials and devices. Applied Materials Today, 12, 366–388.

14. Zhou, X., Yan, Y., Lu, X., Zhu, H., Han, X., Chen, G., & Ren, Z. (2018). Routes for high-performance thermoelectric materials. Materials Today. Volume 21, Issue 9, Pages 974-988.

15. Ma, Z., Wei, J., Song, P., Zhang, M., Yang, L., Ma, J., … Wang, X. (2021). Review of experimental approaches for improving zT of thermoelectric materials. Materials Science in Semiconductor Processing, 121, 105303.

16. Zhang, L., Shi, X.-L., Yang, Y.-L., & Chen, Z.-G. (2021). Flexible thermoelectric materials and devices: From materials to applications. Materials Today, 46, 62–108.

17. Shi, Y., Sturm, C., & Kleinke, H. (2018). Chalcogenides as Thermoelectric Materials. Journal of Solid State Chemistry. Volume 270, 273-279.

18. Soleimani, Z., Zoras, S., Ceranic, B., Shahzad, S., & Cui, Y. (2020). A review on recent developments of thermoelectric materials for room-temperature applications. Sustainable Energy Technologies and Assessments, 37, 100604.

19. Jin, H., Li, J., Iocozzia, J., Zeng, X., Wei, P., Yang, C., … Wang, S. (2019). Hybrid Organic–Inorganic Thermoelectric Materials and Devices. Angewandte Chemie International Edition, 58(43), 15206–15226.

20. Chen, Z.-G., Shi, X., Zhao, L.-D., & Zou, J. (2018). High-performance SnSe thermoelectric materials: Progress and future challenge. Progress in Materials Science, 97, 283–346.

21. Pei, J., Cai, B., Zhuang, H.-L., & Li, J.-F. (2020). Bi2Te3-based applied thermoelectric materials: research advances and new challenges. National Science Review, 7(12), 1856–1858.

22. Wolf, M., Hinterding, R., & Feldhoff, A. (2019). High Power Factor vs. High zT—A Review of Thermoelectric Materials for High-Temperature Application. Entropy, 21(11), 1058.

23. Aranguren, Patricia (2018). Bringing Thermoelectricity into Reality || Nanostructured Thermoelectric Chalcogenides. , 10.5772/intechopen.71354(Chapter 1).

24. Li, Shan; Li, Xiaofang; Ren, Zhifeng; Zhang, Qian (2018). Recent Progress on High Performance of Tin Chalcogenides Thermoelectric Materials. Journal of Materials Chemistry A, (), 10.1039.

25. Wei, Tian-Ran; Guan, Mengjia; Yu, Junjie; Zhu, Tiejun; Chen, Lidong; Shi, Xun (2018). How to Measure Thermoelectric Properties Reliably. Joule, (), S2542435118305117–.

26. Zhang, Yanliang (2018). Thermoelectric Advances to Capture Waste Heat in Automobiles. ACS Energy Letters, (), 1523–1524.

27. Li, X., Chang, L., Chen, Q., Wang, Y., Wang, C., Wang, J., … Jia, X. (2021). Synthesis and characterization of non -stoichiometric SrTiO2.8 thermoelectric materials at high temperature and high pressure. Ceramics International, 47(12), 17627–17632.

28. Nakhowong, Chalida; Sumpao, Teerawut; Seetawan, Tosawat (2013). Synthesis and Characterization of Mg₂Si Thermoelectric Material. Advanced Materials Research, 802(), 213–217.

29. T. Radhika[a*] , r. J. Ramalingam[b*] , p. T. Hasna[a] , a.m. tawfeek[b*] , shaban r. M. Syed[b] , h. Al-lohedan[c] , d. M. Al-dhayan[c] (2019). Synthesis, structural characterization and thermoelectric properties of sr2 (srn-1tino3n+1) n-type ceramic materials, Journal of Ovonic Research,Vol. 15, No. 5, 315 – 323.

30. Huang, Gang; Lv, Chuncheng; He, Junxi; Zhang, Xia; Zhou, Chao; Yang, Pan; Tan, Yan; Huang, Hao; Arenal, Raul (2020). Study on Preparation and Characterization of Graphene Based on Ball Milling Method. Journal of Nanomaterials, 2020(), 1–11.

31. Seong-Bae Kim; Si-Jin Kim; Chang-Ha Kim; Woo-Seong Kim; Kyung-Won Park (2011). Nanostructure cathode materials prepared by high-energy ball milling method. , 65(21-22), 3313–3316.

32. H. J. Fecht; E. Hellstern; Z. Fu; W. L. Johnson (1990). Nanocrystalline metals prepared by high-energy ball milling. , 21(9), 2333–2337.

33. Casallas Caicedo, Francy Mayoli; Vera LÃ³pez, Enrique; Agarwal, Arvind; Drozd, Vadym; Durygin, Andriy; Franco Hernandez, Alexander; Wang, Chunlei (2020). Synthesis of graphene oxide from graphite by ball milling. Diamond and Related Materials, 109(), 108064–.

34. L.B Kong; J Ma; W Zhu; O.K Tan (2001). Preparation and characterization of PLZT ceramics using high-energy ball milling. , 322(1-2), 0–297.

35. Shun Wang,[*a] Weipeng Guan,[a] Dekun Ma,[a] Xian Chen,[a] Li Wan,[b] Shaoming Huang*[a] and Jichang Wang(2009), Synthesis, characterization and optical properties of flower-like tellurium, (). . CrystEngComm, 12(1), – .

36. Marjorie C. Zambonino;Ernesto Mateo Quizhpe;Francisco E. Jaramillo;Ashiqur Rahman;Nelson Santiago Vispo;Clayton Jeffryes;Si

Amar Dahoumane; (2021). Green Synthesis of Selenium and Tellurium Nanoparticles: Current Trends, Biological Properties and Biomedical Applications . International Journal of Molecular Sciences, (), –.

37. Liu, Jian-Wei; Xu, Jie; Hu, Wei; Yang, Jin-Long; Yu, Shu-Hong (2016). Systematic Synthesis of Tellurium Nanostructures and Their Optical Properties: From Nanoparticles to Nanorods, Nanowires, and Nanotubes. ChemNanoMat, 2(3), 167–170.

38. Zhang, R., Tao, C.-A., Chen, R., Wu, L., Zou, X., & Wang, J. (2018). Ultrafast Synthesis of Ni-MOF in One Minute by Ball Milling. Nanomaterials, 8(12), 1067.

39. Yang, L., Zhang, N., Yuan, Y., Cao, X., & Xiang, B. (2018). Thermal performance of stearic acid/carbon nanotube composite phase change materials for energy storage prepared by ball milling. International Journal of Energy Research, 43(12), 6327–6336.

40. Sibul, R., Kibena-Põldsepp, E., Ratso, S., Kook, M., Käärik, M., Merisalu, M., … Tammeveski, K. (2018). Nitrogen-doped carbon-based electrocatalysts synthesised by ball-milling. Electrochemistry Communications, 93, 39–43.

41. Abu-Oqail, A., Wagih, A., Fathy, A., Elkady, O., & Kabeel, A. M. (2018). Effect of high energy ball milling on strengthening of Cu-ZrO2 nanocomposites. Ceramics International.

42. Witting, I. T., Chasapis, T. C., Ricci, F., Peters, M., Heinz, N. A., Hautier, G., & Snyder, G. J. (2019). The Thermoelectric Properties of Bismuth Telluride. Advanced Electronic Materials, 5(6), 1800904.

43. Zhang, Q., Guo, Z., Tan, X., Mao, L., Yin, Y., Xiao, Y., … Jiang, J. (2020). Effects of AgBiSe2 on Thermoelectric Properties of SnTe. Chemical Engineering Journal, 124585.

44. Saleemi, Mohsin; Toprak, Muhammet S.; Li, Shanghua; Johnsson, Mats; Muhammed, Mamoun (2011). Synthesis, processing, and thermoelectric properties of bulk nanostructured bismuth telluride (Bi2Te3). , 22(2), 725–0.

45. Wang, Wen-ting; Zheng, Zhuang-hao; Li, Fu; Li, Cao; Fan, Ping; Luo, Jing-ting; Li, Bo (2018). Synthesis process and thermoelectric properties of n-type tin selenide thin films. Journal of Alloys and Compounds, (), S0925838818321315–.

46. Y.Y. Wang; K.F. Cai; X. Yao (2011). Facile synthesis and characterization of SnTe films. , 258(2), 0–922.

47. Jiang, Qinghui; Hu, Huishan; Yang, Junyou; Xin, Jiwu; Li, Sihui; Viola, Giuseppe; Yan, Haixue (2020). High Thermoelectric Performance in SnTe Nanocomposites with All-Scale Hierarchical Structures. ACS Applied Materials & Interfaces, (), acsami.0c03349–.

48. Wang, Hongchao; Wang, Teng; Hwang, Junphil; Su, Wenbin; Kim, Hoon; Zhai, Jinze; Wang, Xue; wang, chunlei; Kim, Woochul (2018). Optimization of peak and average figures of merits for In & Se co-doped SnTe alloys. Inorganic Chemistry Frontiers, (), 10.1039.C7QI00781G–.

49. Guo, Xuming; Chen, Zhiyu; Tang, Jing; Zhang, Fujie; Zhong, Yan; Liu, Hangtian; Ang, Ran (2020). Thermoelectric transport properties in Bi-doped SnTeâ□“SnSe alloys. Applied Physics Letters, 116(10), 103901–.

50. Gupta, Ravena; Kumar, Naveen; Kaur, Prabhjot; Bera, Chandan (2020). Theoretical model for predicting thermoelectric properties of Tin chalcogenides. Physical Chemistry Chemical Physics, (), 10.1039.D0CP03117H–.